5-2-2009

CHO-human hybrid cells as models for human chromosome non-disjunction

Elizabeth Balconi Evans

CHO-HUMAN HYBRID CELLS AS MODELS FOR HUMAN CHROMOSOME NON-DISJUNCTION

By

Elizabeth Balconi Evans

A Thesis
Submitted to the Faculty of
Mississippi State University
in Partial Fulfillment of the Requirements
for the Degree of Master of Science
in Biological Sciences
in the Department of Biological Sciences

Mississippi State, Mississippi

May 2009

CHO-HUMAN HYBRID CELLS AS MODELS FOR HUMAN CHROMOSOME NON-DISJUNCTION

By

Elizabeth Balconi Evans

Approved:

Dwayne A. Wise Professor of Biological Sciences (Director of Thesis)	Donna Gordon Assistant Professor of Biological Sciences (Committee Member)
Marijo Kent-First Associate Professor of Biological Sciences (Committee Member)	Gary Ervin Associate Professor of Biological Sciences (Graduate Coordinator of the Department of Biological Sciences)

Gary L. Myers
Dean of the College of Arts and Sciences

Name: Elizabeth Balconi Evans

Date of Degree: May 2, 2009

Institution: Mississippi State University

Major Field: Biological Sciences

Major Professor: Dr. Dwayne A. Wise

Title of Study: CHO-HUMAN HYBRID CELLS AS MODELS FOR HUMAN CHROMOSOME NON-DISJUNCTION

Pages in Study: 80

Candidate for Degree of Master of Science

We have used Chinese hamster ovary (CHO)-human hybrid cells containing chromosomes 16, 18, X, or 21 to test the ability of human kinetochores to successfully bind to spindle microtubules and to be distributed to the daughter cells. We have established the intrinsic rate of non-disjunction among these chromosomes and compared these rates with those in cells presented with mitotic challenges. Cells were grown on culture slides, fixed and processed for immunofluorescence and fluorescence *in situ* hybridization (FISH). Daughter pairs were identified by staining with anti-α-tubulin to identify midbodies. Human centromere DNA probes were used for FISH in order to test for the successful passage of human kinetochores to daughter cells. Our data indicate that different human kinetochores vary in their ability to properly engage the spindle and to be successfully distributed. In addition, mitotic challenges have been shown to affect the rate of non-disjunction.

DEDICATION

This thesis is dedicated to all my family and friends who have supported me throughout this endeavor. I would like to especially thank my parents, Greg and Lori Evans, my sister, Stephanie, my brother, Michael, and my grandparents, Carlton and Mildred Rone. I would also like to dedicate this in memory of my grandparents, Robert and Rita Evans.

ACKNOWLEDGEMENTS

I would like to express my sincere gratitude to all those who assisted in the completion of this thesis. I would like to especially thank Dr. Dwayne Wise, my major professor, for guiding me through my graduate education and helping me realize my potential as a scientific researcher. I would like to thank my committee member, Dr. Donna Gordon and Dr. Marijo Kent-First, for their support and guidance throughout my graduate experience. I would like to thank William Monroe and Amanda Lawrence at the Electron Microscopy Center for their instruction and guidance using the confocal microscope. In addition, I would like to thank Clara Esteban Perez for the time and effort she spent in teaching me FISH. I would also like to thank Stephanie Evans, Dr. Chris Brooks and Dr. Russell Stocker for their help with my statistical analysis. Finally, I would like to thank my family and friends who have always been there supporting me in all my endeavors.

TABLE OF CONTENTS

LIST OF TABLES

Page

LIST OF FIGURES

Page

CHAPTER I

INTRODUCTION

Chromosome Non-disjunction

Meiotic Non-disjunction

Meiotic non-disjunction occurs when homologous chromosomes fail to segregate properly to opposite spindle poles and results in gametes with aberrant chromosome numbers. When a normal gamete fuses with a gamete with an extra chromosome the result is a trisomic zygote. Chromosomal trisomies occur in more than fifty percent of spontaneous abortions during the first trimester of pregnancy (Hassold et al. 2007). The three basic results of non-disjunction are: non-disjunction that affects all chromosomes, non-disjunction that affects groups of chromosomes, and non-disjunction that affects individual chromosomes (Hassold et al. 2007). Aneuploidy in humans is a significant cause of spontaneous abortions and mental and physical retardation.

Unequal distribution of chromosomes results in anueploid cells: cells in which the chromosome number is not an even multiple of the haploid number for the species. Aneuploidy in germ cells results in genetic disorders such as Down syndrome (trisomy 21), Edwards syndrome (trisomy 18), and Patau syndrome (trisomy 13). In addition, aneuploidy accompanies tumors and other cancers. Abnormal chromosome number is

associated with malignant tumor cells, and it has also been linked to cell transformation (Cimini et al. 2001). Aneuploidy can be caused by non-disjunction in meiosis I, meiosis II, and in mitosis.

Sex chromosome aneuploidies are found in most of the chromosome abnormalities in human live births. These abnormalities have been linked to meiotic I and meiotic II chromosome non-disjunction. Maternal meiosis I errors are more frequent than meiosis II errors in XXX females. However, nearly fifty percent of XXY male are derived from non-disjunction at paternal meiosis I (Hall et al. 2006). Thomas et al. studied the human chromosome X map using the map^{+} program and found that meiosis I errors have been linked to a decrease in recombination. However, when comparing the non-disjunction linkage map to a standard map they found that aberrant recombination was not involved in transitional meiosis I non-disjunction (Thomas et al. 2001). Non-disjunction occurring during paternal meiosis II results in males with XYY sex chromosomes. In individuals with Turner syndrome (XO), it is not possible to determine the stage of meiosis at which the non-disjunction occurred. However, the source of the non-disjunction can be determined. Seventy to eighty percent of sex chromosome monosomy is caused by a loss of a paternal chromosome. Non-disjunction of autosomal chromosomes can be linked to both paternal and maternal meiotic errors (Hall et al. 2006).

A type of non-disjunction syndrome that is observed in human is trisomy. Trisomies of each chromosome have been observed in spontaneous abortuses. The most frequent trisomies observed were those of chromosomes 13, 14, 15, 16, 18, 21 and 22. Double trisomies have not been reported for chromosomes 1, 3, and 19, but have been

reported for chromosomes 9 and 21, 15 and 22, 8 and 21, 2 and 8, 20 and 22, and 18 and 22. Meiosis I errors were reported for double trisomies for chromosomes 15 and 22, and 8 and 21. Meiotic I and meiotic II errors were found in chromosomes 18 and 22. Chromosome 21 was the only chromosome in which tetrasomy has been observed. Increased maternal age has been linked to the increase in double trisomies compared to single trisomies (Diego-Alvarez et al. 2005).

During spermatogenesis, chromosome 21 and the sex chromosomes showed an increased frequency of aneuploidy (Martin and Rademaker 1999). Non-disjunctions have been found in similar acrocentric chromosomes such as 13, 14, 15, 21, and 22. (Hassold et al. (2007) have also found that meiosis I errors are common in trisomy 16, and meiosis II errors are common in trisomy 18. There are three basic principles for non-disjunction in humans: most non-disjunction occurs during oogenesis, maternal meiosis I errors are more common than meiosis II errors, and non-disjunction increases with maternal age. Errors in cohesion of sister chromatids, pairing and synapsis of homologs and recombination between homologs during prophase have been proposed to lead to chromosome missegregation (Hassold et al. 2007).

In spontaneous abortuses, acrocentric chromosomes are found in one-third of trisomies. Acrocentric chromosomes such as chromosomes 13, 15, 21, and 22 showed an increased frequency of disomy when compared to metacentric chromosomes, such as chromosome 16, 18, and 20. Martin and Rademaker (1999) studied the frequencies of non-disjunction products in human sperm cells. They found that there was an equal

frequency of disomy for most autosomes; however there was a significant increase for chromosome 21 and the sex chromosomes. In addition, they found that there was a significant increase of non-disjunction for chromosome 22 (Martin and Rademaker 1999).

Mitotic Non-disjunction

Bakou et al. (2002) studied cytokinesis-blocked lymphocytes in two different age groups. They found that twenty percent of cells were anueploid for chromosome X in lymphocyte cultures of 47-50 years old women, indicating that mitotic aneuploidy increases with age. They also found that malsegregation of chromosome X was more frequent than was that of chromosome Y. Likewise, chromosome non-disjunction occurred randomly and independently for each autosome (Bakou et al. 2002). Carere et al. (1999) found that chromosome X was more likely than were autosomes to be lost during growth *in vitro*. In addition, chromosome X was more likely to non-disjoin at a higher frequency than chromosomes 7 and 18 (Carere et al. 1999). In an analysis of chromosomes X and 18, approximately nine percent of cells showed malsegregation of both chromosome X and chromosome 18. This suggests that there is a defect in the reliability of the mitotic process in some chromosomes (Carere et al. 1999).
Cimini et al. (1999) compared mitotic loss and non-disjunction of chromosome 7 and 11 between ana-telophase and binucleated cells of human primary fibroblasts. They found that the malsegregation rates observed in nocodazole-treated binucleated cells were lower than those in ana-telophases (Cimini et al. 1999). Cimini et al. (2002) established that in ana-telophase of cells released from a nocodazole-induced-mitotic arrest, loss of a single

sister was more frequent than loss of both sisters. In addition, they found that the frequency of lagging chromosomes for all 23 chromosome pairs was four and one-half percent, and in cells released from a nocodazole-induced-mitotic arrest the frequency was approximately forty-one percent. Furthermore, multiple lagging chromosomes were found in approximately thirty-three percent of anaphase cells (Cimini et al. 2002). These data indicated that mitotic perturbations lead to malsegregation of chromosomes.

Thompson and Compton (2008) used live cell video microscopy to examine the mechanism of chromosome aneuploidies in human tumor cell lines with chromosome instability. They compared five cells lines, two chromosomally stable cell lines (HCT116 and RPE-1) and three chromosomally unstable cell lines (HT29, MCF-7 and Caco2). They found that in the HCT116 cell line, less than ten percent of cells had mitotic defects and these defects were lagging chromatids at anaphase and chromatin bridges. In the chromosomally unstable cell lines, lagging chromatids were observed in twenty-four percent of cells in cell line HT29, forty-two percent in cell line MCF-7, and seventy-five percent in cell line Caco2. They then used a microtubule perturbation drug, nocodazole, to try to increase the incidence of lagging chromosomes in cell lines HTC116 and RPE-1. They found that there was an increase in the number of lagging chromosomes and these were merotelically attached. In HTC116 cells, chromosome missegregation was found more often in cells that were recovered from monastrol than in cells recovered from nocodazole, and the maximum difference of missegregation between these two drugs occurred five to seven days after mitotic recovery. In cell lines RPE-1 and HTC116, chromosome missegregation in untreated cells was approximately 0.025%, whereas in cells recovered from monastrol or nocodazole, chromosome missegregation increased to

approximately 0.6%-0.8%. They found that the missegregation rate per chromosome in the tumor cells lines ranged from approximately 0.3% to 1.0% (Thompson and Compton 2008).

Several mechanisms can lead to chromosome non-disjunction. These mechanisms include disruption of the cell cycle, disruption in the spindle assemble checkpoint, and disruption in kinetochore-microtubule attachment. We will discuss these mechanisms below.

The Cell Cycle

Mitosis is the process that separates copies of chromosomes equally into daughter nuclei. The centrosome is the organizing center for microtubules and the mitotic spindle poles. During interphase, the centrosome pair is located near the nucleus, and during mitosis it forms the spindle poles. In somatic cells, the centrosome is replicated during S phase of interphase and at the end of S phase; duplicated chromosomes remain in close association with one another (Sun and Schatten 2007). These sister chromatids are connected to each other by the protein, cohesin, which is cleaved at anaphase by the enzyme, separase. During early mitosis, the nuclear envelope breaks down and the sister chromatids attach to microtubules that emanate from the spindle poles. During metaphase, the plus ends of the microtubules attach to the kinetochores and align the chromatids along the metaphase plate. Kinetochores must capture microtubules and attach themselves to opposite poles before anaphase can occur (Tanaka and Desai 2008). Nicklas (1988) showed that it only takes one chromosome to trigger spindle formation and in these cases mitosis was completed. During anaphase, the sister chromatids

separate and are “pulled” to opposite spindle poles. Anaphase A is characterized by the movement of chromatids to the spindle poles accompanied by the disassembly of microtubules, and anaphase B is characterized by the separation of spindle poles by the sliding of overlapping microtubules in the midzone. After anaphase and telophase, the complete sets of chromosomes are then enclosed in two new daughter cells and the nuclear envelope reassembles.

The centrosome’s main function is the organization of spindle microtubules into spindle poles. This mediates the separation of chromosomes into each daughter pair. Malfunctions in centrosome duplication and structure can lead to multipolar spindles, accompanied by abnormal chromosome segregation and aneuploidy and subsequent tumor formation and cancer. The nuclear mitotic apparatus protein (NuMA) is an essential cell cycle-dependent centrosome-associated protein that is distributed to each centrosome during early mitosis (Sun and Schatten 2007). It is responsible for minus-end binding and stabilization of the side of the centrosome facing the chromosomes. This results in cross-linking of the spindle microtubules, which is essential for organization and stabilization of the spindle poles. However, the centrosome is not required for spindle pole formation. For instance, human gametes can establish bipolar spindles in the absence of centrosomes, and somatic cells can use a centrosome-independent pathway to produce spindles when the centromere is absent (Sun and Schatten 2007).

There are many checkpoints that monitor the progression of mitosis and spindle pole assembly. The checkpoint that is most relevant to our study of non-disjunction is the spindle assemble checkpoint (SAC) because it monitors the connection to, and maintenance of, microtubules to kinetochores.

Spindle Assembly Checkpoint (SAC)

The cell cycle is controlled by several checkpoints. These checkpoints monitor microtubule attachment to the kinetochore and the tension that results from forces exerted on the kinetochore (Sudakin and Yen 2007). Chromosome separation is controlled by the metaphase-anaphase transition checkpoint. Sister chromatids are linked together by a protein called cohesin. Stimulation of the anaphase-promoting complex by the M-phase cyclin-Cdk complex allows the progression through this checkpoint by destroying the cohesin and other cyclin proteins that hold the chromatids together. This destruction of proteins triggers segregation and spindle disassembly. The spindle checkpoint prevents chromosome segregation by delaying anaphase if the microtubules are not stably attached to the kinetochores and the tension is not the same as that on metaphase aligned chromosomes. In the event that the checkpoints are inhibited, the cells will be anueploid (contain multiple copies of a chromosome) when they exit mitosis. However, Cimini et al. (2001) showed that when cells are exposed to high doses of spindle poisons they bypass the mitotic checkpoints, which suggests that the checkpoint is not as efficient as was thought (Cimini et al. 2001). When mice were genetically engineered to gain or lose chromosomes because of a defect in mitosis, it resulted in heterozygous mice with one functional copy of the checkpoint protein, CENP-E. Ten percent of aged (19-21 months) heterozygous mice developed splenic lymphomas and were shown to have an increase in lung tumors. In addition to these findings, CENP-E has been shown to inhibit tumorigenesis in animals that lack the tumor suppression gene known as *p19/ARF*. The spindle checkpoint protein, Mad2, has been shown to be inhibited by the retinoblastoma pathway, which causes over-expression of Mad2. This pathway was found to be

compromised in most human cancers (Pellman 2007). SAC monitors kinetochore attachment, but in order for microtubules to connect to kinetochores many proteins must be present. Errors in kinetochore attachment associated with the SAC result in aneuploid cells.

Aneuploidy results from small changes in the mitotic checkpoints rather than complete inactivation of the checkpoints. Epigenetic silencing (gene inactivation) can also cause a reduction in the level of expression of the checkpoint proteins (Cimini and Degrassi 2005). Merotelic kinetochores are unique in that they are not detected by the checkpoint. Merotelic kinetochore attachment results when microtubules attach the kinetochore of only one sister chromatid to both spindle poles. This leads to missegregation of the chromatids which results in aneuploidy of the cell. Merotelic kinetochore attachment can result in lagging chromosomes, which are chromosomes that are left at the spindle equator after anaphase onset. Lagging chromosomes were found in 0.5-5% of anaphase cells in humans and mammalian cell cultures (Cimini et al. 2003). Anaphase does not proceed as normal: the sister chromosome is pulled in the opposite direction because it is attached to microtubules at the opposite pole. In addition to merotelic kinetochores, aneuploidy can be caused by separated sister chromatids moving to the same pole, which is termed 'sister chromosome non-disjunction', which happened at a higher frequency than lagging chromosomes (Salmon et al. 2005). Merotelic attachment of the kinetochore to microtubules is a common mechanism that is found in tumor cell lines expressing aneuploidy (Thompson and Compton 2008). Cimini et al. (1999) also found that merotelic attachment increases in mitotic cells when they are exposed to drugs such as taxol and nocodazole that perturb microtubule turnover.

Kinetochore Attachment

Initial Attachment

The kinetochore is a large complex consisting of multiple proteins and the underlying DNA base sequence. The kinetochore assembles on the centromere DNA sequence of the chromosomes during mitotic entry. It functions to attach the chromosome to the spindle in order for proper segregation of the chromosomes. During metaphase, the kinetochores attach to the microtubules by capturing them when "whole" microtubules are present (Nicklas 1988). Mammalian kinetochores have between fifteen and twenty-five plus-end-microtubule-attachment sites on the outer plate. Once the kinetochore attaches to the microtubule, it is "pulled" to the opposite poles. The sister kinetochores face opposite directions so that when one kinetochore attaches to a microtubule from one spindle pole it causes the other sister kinetochore to face the opposite direction and to attach to the opposite spindle (Cimini et al. 2003). After the kinetochores achieve bi-orientation, the chromosome arms are aligned at the metaphase plate (Tanaka and Desai 2008). However, not all chromosomes achieve bi-orientation of their kinetochores.

In some cases, the kinetochores are not facing a pole and the microtubules from one pole can attach to both sister chromosomes. The condition is defined as monopolar orientation and results in one daughter cell receiving both chromosomes. In cases in which the kinetochore is not attached correctly, then the kinetochore-spindle complex must be re-oriented to achieve proper bi-orientation of the sister kinetochores before

anaphase can continue (Tanaka and Desai 2008). There are several proteins that are associated with the kinetochore that aid in microtubule attachment.

Maintenance of Attachment

The Ndc80 complex is an outer kinetochore constituent that is conserved from yeast to humans. It directly interacts with microtubules and, when depleted, chromosome segregation is aberrant. Biochemical analysis and electron microscopy have shown that the Ndc80 complex interacts with the microtubule lattice, explaining its requirement for kinetochore binding to the microtubule (Tanaka and Desai 2008).

CENP-E is a protein found on the kinetochore during mitosis which assists in establishing bipolar attachment of chromosomes that have monopolar attachment. CENP-E establishes tension on the microtubules to allow the chromosomes to move to the spindle poles during anaphase (Yen et al. 2004). In metazoan cells, CENP-E transports mono-oriented kinetochores away from one spindle and towards the metaphase plate by moving along the microtubules that were already attached to bi-orientated kinetochores (Tanaka and Desai 2008).

Another protein necessary for establishing bi-orientation of sister kinetochores is Aurora B kinase. This kinase eliminates the kinetochore-spindle connections that do not generate tension between the two sister kinetochores. Inhibition of Aurora resulted in syntelic attachment, in which both sister kinetochores were attached to the same spindle pole, and merotelic attachment, in which one sister kinetochore was attached to both spindle poles. Aurora B functions in avoiding or correcting merotelic attachment (Tanaka and Desai 2008). Topoisomerase II localizes and separates entangled DNA

strands that result from replication or transcription. Aurora B requires topoisomerase II for its kinase activity; therefore depletion of topoisomerase II decreases the kinase activity of Aurora B kinase. In control HeLa cells, Aurora B activity was present during prometaphase but down-regulated during metaphase. However, in cells in which topisomerase II was depleted Aurora B activity was decreased in prometaphase and more than sixty percent of cells had syntelic kinetochore attachment. This shows that topisomerase II was required for amphitelic kinetochore attachment. This further indicated that topisomerase II was required for regulating Aurora B kinase activity at the centromere of chromosomes (Coelho et al. 2008). In order for microtubules to attach to kinetochores, motor proteins must be present.

There are several motor proteins, such as dynein and kinesin that are associated with microtubules. Dynein is located at the kinetochore and along microtubules and is associated with the spindle poles during mitosis. These motor proteins move along microtubules by interacting with tubulin subunits found in microtubules. Motor proteins hydrolyze ATP and convert chemical energy into mechanical work. Dynein is a motor protein that aids in spindle formation, chromosome attachment, and SAC protein removal. In addition, it assists in chromosome movement during anaphase (Varma et al. 2008). Dynein has been shown to focus microtubule ends into spindle poles and is required for organizing microtubules into asters (Fant et al. 2004). During prometaphase, levels of dynein are high, but decrease when the kinetochore binds to spindle microtubules. When dynein was blocked by microtubule depolymerization and anti-dynein antibody, dynein was removed along with the spindle assembly checkpoint

proteins (Varma et al. 2008). Kinesin is also a motor protein that assists in microtubule-kinetochore attachment.

There are three subfamilies of kinesin-related proteins that have been found to associate with mitotic spindle assembly. These subfamilies are: KIN C, KIN N, and KIN I. The motor activity of KIN N is located at the amino terminus, the motor activity of KIN C is located at the carboxyl-terminus and the motor activity of KIN I is located in the center of the protein sequence. KIN C moves towards the minus-ends of microtubules, whereas KIN I and KIN N move towards the plus-ends. KIN C has been shown to induce cross-linking of microtubules. An example of a KIN C motor protein is the Ncd motor protein that is found in *Drosophila*. Ncd has been shown to play a direct role in spindle microtubule organization and transporting other microtubule-organizing proteins to the minus end of the microtubule (Fant et al. 2004).

BimC-related motor proteins Eg5 in vertebrates and KLP61F in *Drosophila* is one type of KIN N motor proteins that are associated with the spindle pole during mitosis. The BimC-related motor proteins move anti-parallel microtubules apart. During mitosis these proteins push microtubules in opposite directions which move the minus end outwards which drives the separation of the centrosomes. In addition, BimC-related motor proteins play a role in focusing spindle microtubules at the pole (Fant et al. 2004).

Three examples of KIN I proteins are: MCAK in humans and KLP59C and KLP10A in *Drosophila.* These proteins do not move and remain bound to the kinetochore. Their function is the help with depolymerization of the plus end of the spindle microtubules. KLP10A is a newly identified KIN I motor protein found in *Drosophila*. It plays a role in spindle pole development by depolymerizing the minus end

of microtubules. It has been suggested that KLP10A helps in shortening kinetochore fibers leading to chromosome movement to the poles during anaphase (Fant et al. 2004). Once the motor proteins assist the microtubules in attaching to the kinetochore, stability of the microtubule-kinetochore complex must be achieved.

Inter-kinetochore spacing and the stability of microtubule attachment determines proper microtubule attachment to kinetochores. Varma et al. (2008) used dynein tail-expressing cells to determine the effects of dynein on the stability of the kinetochore-microtubule attachment. They found that there was a decrease in the number of microtubule bundles in cold-resistant kinetochores with tail-expressing dynein compared to controlled kinetochores resulting in decreased stability. In addition, Varma et al. (2008) found that there was a reduction in the inter-kinetochore spacing between kinetochore pairs of controlled aligned chromosomes and kinetochore pairs of aligned chromosomes in dynein tail-expressing cells. This showed that there was a sixty-nine percent reduction in tension between the two cells. Varma et al. (2008) also found that there was mis-orientation of aligned kinetochores in the dynein tail-expressing cells. Similarly, cells with dynein-expressing tails had an increase in the number of unattached or mono-attached kinetochores. This demonstrated that dynein was used for the removal of itself and other kinetochore proteins during microtubule attachment. Additionally, dynein along with Kif18A facilitated in the regulation of chromosome oscillations in metaphase (Varma et al. 2008).

Clearly, the causes of chromosome non-disjunction are not fully understood. Several studies have shown that chromosome non-disjunction in mitosis accompanies tumor formation and cancer. In addition, aneuploidy as a result of meiotic non-

disjunction has been found in spontaneous abortuses. Many scientists have sought to understand the mechanism of non-disjunction, but it has not been fully explicated. Determining how non-disjunction occurs has the potential to aid in treatments of tumors and other cancers and to prevent inherited anueploid conditions.

There are several methods for detecting chromosomal aneuploidies. These include karyotyping, chromosome sorting, human hybrid cell lines, and fluorescence in situ hybridization. These will be discussed below.

Detection of Chromosome Non-disjunction

Karyotyping

Karyotyping is a process in which cells are studied in order to determine chromosomal abnormalities such as non-disjunction. Karyotyping can use amniotic fluid, bone marrow and other fluids samples to determine chromosomal abnormalities that lead to cancer. The karyotype is the complete characteristics of all the structural features of mitotic metaphase chromosomes and homologous segments in meiotic pairing. Structural features that can be determined by karyotyping are chromosome number, size and morphology. Two types of karyotyping are spectral karyotyping and electrophoretic karyotyping.

Spectral karyotyping can be used to identify different chromosomes using a palette of 24 different colors. Spectral karyotyping uses fluorescence in situ hybridization to label chromosomes with different colors which can then be identified when a computer separates the different emission spectrum. This allows the complete

human genome to be studied at one time through the display of different colors. Chromosome deletions, translocations, insertions and additions can be identified using spectral karyotyping. This can help in determining the cause and identifying the types of cancers (Zhao et al. 2001).

Electrophoretic karyotyping uses pulsed field gel electrophoresis to visualize whole chromosomes from unicellular organisms. Pulsed field gel electrophoresis extends the upper limit to at least 5.7 megabases, which is the size range of chromosomes of most bacteria, fungi, and protozoa. Restriction enzymes produce chromosome fragments that can be separated by pulsed field gel electrophoresis. This data can then be combined to determine the accurate size of chromosomes. Another way to detect chromosome non-disjunction is cell and chromosome sorting.

Cell and Chromosome Sorting

Cell sorting and chromosome sorting are specialized types of flow cytometry which are techniques used to count, examine and sort microscopic particles suspended in a stream of fluid. The cells or chromosomes are stained with a fluorescence dye. The cells or chromosomes are then put into a cytometer that shoots a droplet through a detector with a laser light source and a photocell to measure the fluorescence drop by drop. The investigator can analyze the data to determine the distribution of cell or chromosome sizes in a population, and the DNA content of the cells. Cell and chromosome sorting can be performed in a human-hybrid cell line which is a model cell line to study chromosome non-disjunction.

Human Hybrid Cell Lines

Human hybrid cell lines were established in order to study biological functions of humans in culture cells. We will use various Chinese hamster ovary (CHO)-human hybrid cell lines. This cell line fuses CHO cells with lymphocytes, and through a series of selective media the human chromosome is retained in the CHO cells. In order to select for the hybrid cells, the parent cells (in our case CHO cells) must be deficient for hypoxanthine-guanine phosphoribosyl transferase ($HGPRT^-$) or thymidine kinase (TK^-). This blocks the salvage pathway in which purine synthesis or pyrimidine synthesis is blocked by aminopterin, which is included in the HAT selective medium. Once the parent cell and the lymphocyte are hybridized, the parent cells and the mortal lymphocytes die because they are not being selective for in the selective medium, leaving only cells containing the HGPRT gene from lymphocytes. The hybrid cells will then survive and proliferate in HAT medium containing hypoxanthine, aminopterin, and thymidine supplements. Hybrid cells usually contain one to a few human chromosomes, which can be advantageous in mapping loci to specific chromosomes.

Fluorescence *in situ* Hybridization (FISH)

Fluorescence *in situ* hybridization is a technique used to directly analyze chromosomal aberrations. The use of chromosome centromeric-specific probes allows the determination of the distribution of chromosomes between the daughter pair by analyzing the hybridization signal. *In situ* probes consist of cloned DNAs that hybridize to their complementary DNA strand. These probes are labeled with a fluorescent label that will allow detect of the chromosome. An important advantage of FISH is that is

allows for the detection of malsegregation in multiple chromosomes at the same time. FISH probes can be centromere specific, loci specific, or Alu sequence specific. In our study we will use centromere specific probes.

Experimental Perturbation of Chromosome Distribution

Mitosis with Unreplicated Genomes (MUG)

One way to study chromosome non-disjunction in human-hybrid cell lines is by inducing mitosis with unreplicated genomes to produce unreplicated chromosomes in a daughter pair. Mitosis with unreplicated genomes occurs at the onset of S-phase with the exposure of cells to hydroxyurea (HU) and caffeine. HU arrests the cells in S-phase, then with the addition of caffeine, the cell proceeds through mitosis without replicating the chromosomes. Studies with mitotic cells with unreplicated genomes (MUGs) showed that the chromosomes were fragmented, but the kinetochore still bound to the microtubules and aligned along the metaphase plate. This showed that the spindle retained the information necessary to align the chromosomes at the metaphase plate and to divide them equally into daughter cells at anaphase. In addition to fragmented kinetochores, the MUG cells had widespread DNA damage during which the chromatin was spread throughout the cell (Wise and Brinkley 1997).

Taxol

Taxol has been used widely as a first-line chemotherapy agent in the treatment of solid tumors such as ovarian cancer. Taxol inhibits microtubule depolymerization by

binding to β-tubulin. The result in living cells is metaphase arrest. Cells that are treated with taxol are multipolar and contain multiple microtubule asters. If taxol is added to cells after the onset of mitosis, the cells will have a bipolar spindle orientation; however the cells will be halted before the onset of anaphase. In addition, the addition of taxol at the onset of anaphase will delay the onset of anaphase B. Hornick et al. (2008) used live-cell video microscopy in order to observe microtubule behavior in taxol-treated cells as they transition from interphase to mitosis. They found that, after the addition of taxol, cells transitioned into mitosis and assembled aster and multipolar spindles. In addition, they found that aster formation was not a spontaneous event. It occurs as pre-existing microtubules become relocalized into the cell periphery; they then shorten and align at the cell cortex. As they align at the cell cortex, the microtubules curve and become cytoasters. The asters then detach from the cortex and migrate towards the chromosome creating a multipolar cell. However, some of the asters depolymerized before they became incorporated into a spindle pole (Hornick et al. 2008). Hornick et al. (2008) also found that when cells are treated with taxol, the microtubules are released from the centrosome as they enter into mitosis and spindle pole components relocate to microtubules in the cortex and cytoasters. They also found that dynein is not required for cytoaster formation in taxol-treated cells (Hornich et al. 2008).

Ikui et al. (2005) studied the effects of low concentration of taxol on HeLa cells and found that cells treated with low concentrations of taxol escaped the mitotic block because of an inactivation in the SAC. They found that high concentrations of taxol (>20nM) caused mitotic arrest and low concentrations of taxol caused aneuploidy in the cells with an absence in mitotic arrest. In addition, they found that when cells are treated

with concentrations greater than 20nM taxol the cells are arrested in mitosis by the formation of the Mad2-p55CDC complex (Ikui et al. 2005).

Nocodazole

Nocodazole is a widely used chemotherapy agent that increases microtubule depolymerization and halts cells at the G2/M phase transition. It has also been found to increase aneuploidy and polyploidy. Verdoodt et al. (1999) treated PHA-stimulated lymphocytes with 0.04μg/ml and 1.0 μg/ml of nocodazole and found that nocodazole increased the percentage of abnormal metaphase and anaphase compared to total amount of mitotic cells. In addition, they found that on the same slides there was an increase in the amount of apoptotic cells as the treatment time of nocodazole increased. Verdoodt et al. (1999) also found that there was an increase in the mitotic index when cells were treated with nocodazole, and the percentage of polyploidy metaphase cells increased as time in nocodazole increased. They also found that wild-type p53 prevent polyploidy by blocking replication of these polyploidy cells. They found that the percentage of polyploidy cells is approximately the same in apoptotic and non-apoptotic cells before the rereplication cycle. This suggests that G_1/S transition is controlled by p53 (Verdoodt et al. 1999).

Mitotic challenges such as MUG, taxol and nocodazole can expand our knowledge of chromosome non-disjunction by providing incite on how chromosomes are distributed when DNA is fragmented or when microtubule dynamics are disturbed.

Research Objectives

A. Determine the intrinsic rate of mitotic non-disjunction for various human chromosomes in CHO-human hybrid cells.

B. Determine the rate of mitotic non-disjunction for various human chromosomes when they are presented with various mitotic challenges.

C. Determine the patterns of intrinsic rate of mitotic non-disjunction for various human chromosomes in CHO-human hybrid cells.

D. Determine the effect of microtubule perturbations on non-disjunction ratios for various human chromosomes.

CHAPTER II

MATERIALS AND METHODS

Cell Culture Technique

The Chinese hamster/human hybrid cell line GM11979 was grown in Ham's F-12 with 2mM L-glutamine medium with 7% dialyzed fetal bovine serum uninactivated. Cultures were kept in a 37^{o}C incubator with an atmosphere of 5% CO_2.

The Chinese hamster/human hybrid cell line GM10330 was grown in Dulbecco Modified Eagles (high glucose) with 2mM L-glutamine medium with 10% fetal bovine serum uninactivated. In addition 5 x 10^{-4}M azaserine and 1 x 10^{-4}M hypoxanthine supplements were added to the medium. Cultures were kept in a 37^{o}C incubator with an atmosphere of 8% CO_2.

The Chinese hamster/human hybrid cell line GM13535 was grown in Dulbecco Modified Eagles (high glucose) with 2mM L-glutamine medium with 10% fetal bovine serum uninactivated. In addition, 34.5 mg/L of proline supplement were added to the medium. Cultures were kept in a 37^{o}C incubator with an atmosphere of 8% CO_2.

The Chinese hamster/human hybrid cell line GM11130 was grown in Dulbecco Modified Eagles (high glucose) with 2mM L-glutamine medium with 10% fetal bovine serum uninactivated. In addition, 4 x 10^{-7}M aminopterin, 1 x 10^{-4}M hypoxanthine, and 1.6 x 10^{-5}M thymidine supplements were added to the medium. Cultures were kept in a 37^{o}C incubator with an atmosphere of 8% CO_2.

Hydroxyurea (HU) Technique

Cells were treated with 2.2mM hydroxyurea in order to halt the cells in S phase for synchronization. The cells were then released by replating in fresh medium for 14-20 hours. The cells were then plated, fixed, and treated for IF and FISH to determine the intrinsic rate of non-disjunction.

MUG Technique

Cells were treated with trypsin-EDTA and plated on NUNC SlideFlask culture slides. The culture slides were incubated 24 hours. 2mM hydroxyurea (HU) in medium was added to the culture slide and incubated for 20 hours. After 20 hours, 5mM caffeine was added to the culture slide and incubated for 14 hours.

Taxol Technique

Cells were treated with trypsin-EDTA, plated on NUNC SlideFlask culture slides and incubated for 24 hours. After 24 hours 20nM-80nM taxol was added to the medium and incubated for 8-9 hours. After 8-9 hrs the medium was discarded and fresh medium was added for 1-3 hours. The cells were lysed and fixed for FISH and immunofluorescence for various proteins.

Nocodazole Technique

Cells were treated with trypsin-EDTA and plated on NUNC SlideFlask culture slides. The culture slides were incubated for 24 hours and then replaced with 2μM nocodazole in medium for 8-9 hours to arrest cells in mitosis. After 8-9 hours, the cells

where re-incubated in fresh medium for 1-8 hour. The cells were lysed and fixed for FISH and immunofluorescence for various proteins.

Immunofluorescence (IF) Techniques

Carnoy's Solution and Formaldehyde Fixation

For slides that were stained with anti-α-tubulin, the culture slides were removed from the incubator and the slides were immersed in 3:1 methanol: acetic acid for 5 minutes in a -20^{o}C freezer. The slide was immersed in 50ug/ml Trypsin in 0.01M HCl in a 37^{o}C water bath for 5 minutes. The slides were washed twice in 1X PBS for 5 minutes at RTwhile shaking. An addition wash in 50mM $MgCl_2$ in PBS at room temperature was then required. The slide was placed in 1% formaldehyde/ 1X PBS/50mM $MgCl_2$ for 10 minutes. The slide was washed twice in 1X PBS for 5 minutes each. The slide was washed with 0.5% Triton X-100 for 10 minutes. To remove the detergent, three 1X PBS washes for 5 minutes was needed.

Anti-α-Tubulin Staining

The slides were placed face down on a Petri dish containing moistened filter paper and parafilm. Two 50µL drops of 1% BSA and 0.5% sodium azide in PBS were placed on each slide and incubated for 30 minutes at 37^{o}C. After 30 minutes, the 1% BSA and 0.5% sodium azide in PBS was removed with three washes of 1X PBS for 5 minutes each. Two 50µL drops of 1% BSA and 0.5% sodium azide in PBS containing a primary antibody of diluted anti-α-tubulin (1:167 dilution) was added to the slide, and

then they were incubated for 45 minutes at 37°C. The slide was washed three times in 1X PBS for 5 minutes each to dissolve excess antibody. Two 50µL drops of 1% BSA and 0.5% sodium azide in PBS containing a secondary complimentary to the primary was added to the slide, and then it was incubated for 45 minutes at 37°C. The slides were rinsed three times in 1X PBS for 5 minutes each and then used for *in situ* techniques.

Fluorescence *in situ* Hybridization (FISH) Technique

After the slides were processed by IF techniques they were prepared for *in situ* hybridization. The slides were place in a 70% formamide solution at 73°C for 5 minutes. They went through a series of alcohol dehydrations: 70%, 85%, and 100% for 1 minute each. The slides were allowed to air dry in the dark. The appropriate centromere specific probe was prepared using the protocol supplied by Vysis or Rainbow Scientific. The probe solution was vortexed and placed in a 37°C-73°C water bath for 5 minutes. The slide was place on a 40°C-50°C hot plate for 5 minutes. 10µL of the probe solution was added to the slide. A coverslip and parafilm was placed over the probe solution and the slide was incubated in a hybridization chamber at 37°C-42°C for 6-24 hours. After hybridization, the slides were washed in 0.4X SSC/0.3% NP-40 at 70°C-73°C for 2 minutes. A second wash in 0.4X SSC/0.1% NP-40 at room temperature for 1 minute was required.

DAPI Stain

Once the cells have been stained using FISH techniques, the slides were placed in a 1:10,000 dilution of DAPI in PBS for 15 minutes. After 15 minutes, the slides were

washed three times with 1X PBS for 5 minutes each. Coverslips were mounted on the slides using Vetashield mounting medium.

Confocal Microscopy

Confocal microscopy is an optical imaging technique used to construct three-dimensional pictures of a sample. After staining, the slides were observed using a Zeiss LSM laser scanning confocal microscope. Optical sections were taken with 63X and 100X objectives. Fluorescence signals were identified and recorded. In cases where the signal number was difficult to ascertain, the problem was resolved by rotating the three-dimensional digital image to determine the number of signals. If there was still uncertainty, the daughter pair was not counted.

Statistical Analysis

The JMP8 statistical software was used to analyze the data for statistical significance using a nominal logistic regression analysis, which allows for analysis of non-normally distributed data. A nominal logistic regression is used to study data that has categorical dependent variables and independent variables. In our case, we have a categorical dependent variable which is disjunction type (Correct Disjunction vs. Non-disjunction). Our independent variables that help to determine the output are types of chromosome (16, X, 18, or 21) and treatment (intrinsic rate, taxol, or nocodazole).

CHAPTER III

RESULTS

Chromosome 16

The intrinsic rate of non-disjunction for chromosome 16 was determined by using a FISH technique to label the its centromeric region. These signals were then counted in each daugher pair. The daughter pairs were identified by anti-tubulin antibody staining to label the midbodies. Cells were syncronized by using 2.2mM hydroxyurea to halt cells in S phase. Non-disjunction for each chromosome was marked by an unequal distribution of *in situ* signals between each member of a daughter pair. We found that chromosome 16 non-disjoins at a frequency of 25% (n=163) (Figures 1-5, Table 1). The type of non-disjunction that occurred most often for chromosome 16 in unteated cells was a 1:0 ratio (13.6%) (n=90) in which one daughter cell contained one chromosome 16 and the other daughter cell contain no copies of chromosome 16 (Figures 1, 4, 7, 31, Table 1).

Cells containing chromosome 16 were then treated with 20nM taxol and then released for 1 hour. We found that, for cells treated with taxol then released, the rate of non-disjunction for chromosome 16 increased from 25% (n=163) to 29% (n=152) when compared to the intrinsic rate of non-disjunction (Figures 6-12, Table 1). The type of non-disjunction that occurred most often for chromosome 16 when treated with taxol was

a 1:0 ratio (13%) (n=68) which is approximately the same as the intrinsic rate of non-disjunction (Figures 15, Table 1).

Correct disjunction for MUG cells was marked by cells containing one *in situ* signal per daughter pair, since the MUG technique does not allow DNA replication. When cells were treated with the MUG technique and then probed for chromosome 16 it was found that most cells (68%) (n=154) had correct disjunction, with one signal in one cell of a daughter pair (Figures 13 and 14).

Chromosome 18

The intrinsic rate of non-disjunction for chromosome 18 was determined by counting the centromere-specific in situ signals in each daugher pair. The daughter pairs were identified by anti-tubulin antibody staining to label the midbodies. The data showed that chromosome 18 non-disjoins at a frequency of 43% (n=217) (Figures 2, 16-21). The type of non-disjunction frequency most prevalent in unteated cells for chromosome 18 was a 1:0 ratio (18.6%) (n=94) (Figures 34, Table 1).

Cells containing chromosome 18 were then treated with 80nM taxol and then released for 2.5 hours. We found that, for cells treated with taxol then released, the rate of non-disjunction for chromosome 18 decreased from 43% (n=217) to 22% (n=110) when compared to the intrinsic rate of non-disjunction (Figures 6 and 15, Table 1). The type of non-disjunction that occurred most often for chromosome 18 when treated with taxol was a 2:1 ratio with a frequency of 7.9% (n=26) (Figure 15, Table 1).

Chromosome X

The intrinsic rate of non-disjunction for chromosome X was determined by counting the *in situ* signals in each daugher pair. The daughter pairs were determined by anti-tubulin antibody staining to label the midbodies of the daughter pairs. The cells were then probed using the FISH technique with a chromosome X centromere-specific probe. It was found that chromosome X non-disjoins at a frequency of 23% (n=35) (Figures 2 and 23, Table 1). The type of non-disjunction that occurred most often in untreated cells for chromosome X was a 2:1 ratio (11.2%) (n=17) in which one daughter cell contained two chromatids of chromosome X and the other daughter cell contained one chromatid of chromosome X (Figures 1 and 22, Table 1).

Cells containing chromosome X were then treated with 80nM taxol and then released for 2.5 hours. The data showed that, for cells treated with taxol then released, the rate of non-disjunction for chromosome X increased from 23% (n=35) to 32% (n=44) when compared to the intrinsic rate of non-disjunction (Figures 6, 22, and 23, Table 1). The type of non-disjunction that occurred most often for chromosome X when treated with taxol was a 1:0 ratio with a frequency of 19.1% (n=26) (Figures 22, 24 and 25, Table 1).

Cells containing chomosome X were treated with 2μM nocodazole, released for 8 hours, and then probed for chromosome X. We found that nocodazole increased the rate of non-disjunction from 23% (n=35) to 27% (n=41) when compared to the intrinsic rate of non-disjunction, but when compared to cells treated with taxol it decreased the rate from 32% (n=44) to 27% (n=41) (Figures 6, 22, 24 and 25, Table 1). The type of non-

disjunction that occurred most often for chromosome X when treated with noodazole was a 1:0 ratio with a frequency of 9.9% (n=15) (Figures 6, 22, 26 and 27, Table 1).

Chromosome 21

The intrinsic rate of non-disjunction for chromosome 21 was determined by counting the in situ signals in each daugher pair. The daughter pairs were determined by anti-tubulin antibody staining to label the midbodies of the daughter pairs. The cells were then probed using the FISH technique wtih a chromosome 21 centromere-specific probe. It was found that chromosome 21 non-disjoins at a frequency of 23% (n=35) (Figure 2). The type of non-disjunction that occurred most often in untreated cells for chromosome 21 was a 3:2 ratio (11.8%) (n=12) in which one daughter cell contained three chromatids of chromosome 21 and the other daughter cell contained two chromatids of chromosome 21 (Figures 28-30, Table 1).

Interchromosome Comparison

A nominal logistics analysis was performed to determine if any particular chromosome has an effect on distribution (correct disjunction vs. non-disjunction) for cells without a treatment (intrinsic rate). Using the 95% confidence interval, chromosome 16 had a *P*-value of 0.0458, chromosome 18 had a *P*-value of 0.0131 and chromosome 21 had a *P* -value of 0.0208, which implies that there was a significant difference between correct disjunction and non-disjunction among chromosomes. Differences between chromosomes were determined by dividing the non-disjunction frequency of one chromosome by the correct disjunction frequency of another

chromosome to obtain an odds ratio (OR), and if the number is not close to one than it is considered significantly different. Using this method, we compared the intrinsic rate of non-disjunction and found that with chromosome X to chromosome 18 there was a significant difference (OR=2.51) between the non-disjunction of chromosome X and the correct disjunction of chromosome 18, and there was also a significant difference (OR=2.44) between the non-disjunction of chromosomes X and the correct disjunction of chromosome 21. In addition, we found that there was a significant difference (OR=0.43) between the non-disjunction of chromosome 18 and the correct disjunction of chromosome 16 and between the non-disjunction of chromosome 21 and the correct disjunction of chromosome 16 (OR=0.45) (Figures 31 and 32, Table 2) (See Appendix, Figures A.1, A.2, and A.3).

We then tested the effects of the treatments (intrinsic vs. taxol) for each chromosome and found that there was a significant difference for the intrinsic rate of non-disjunction for chromosome 18 ($p=0.0016$) using the confidence interval of 95%. In addition, we found that the intrinsic rate of non-disjunction for chromosome 21 had a significant effect on the distribution of chromosomes ($p=0.0208$) using the confidence interval of 95%. There was not enough evidence to conclude that chromosomes 16 and X had a significant effect on non-disjunction using a 95% confidence interval (See Appendix, Figures A.1, A.2, and A.3).

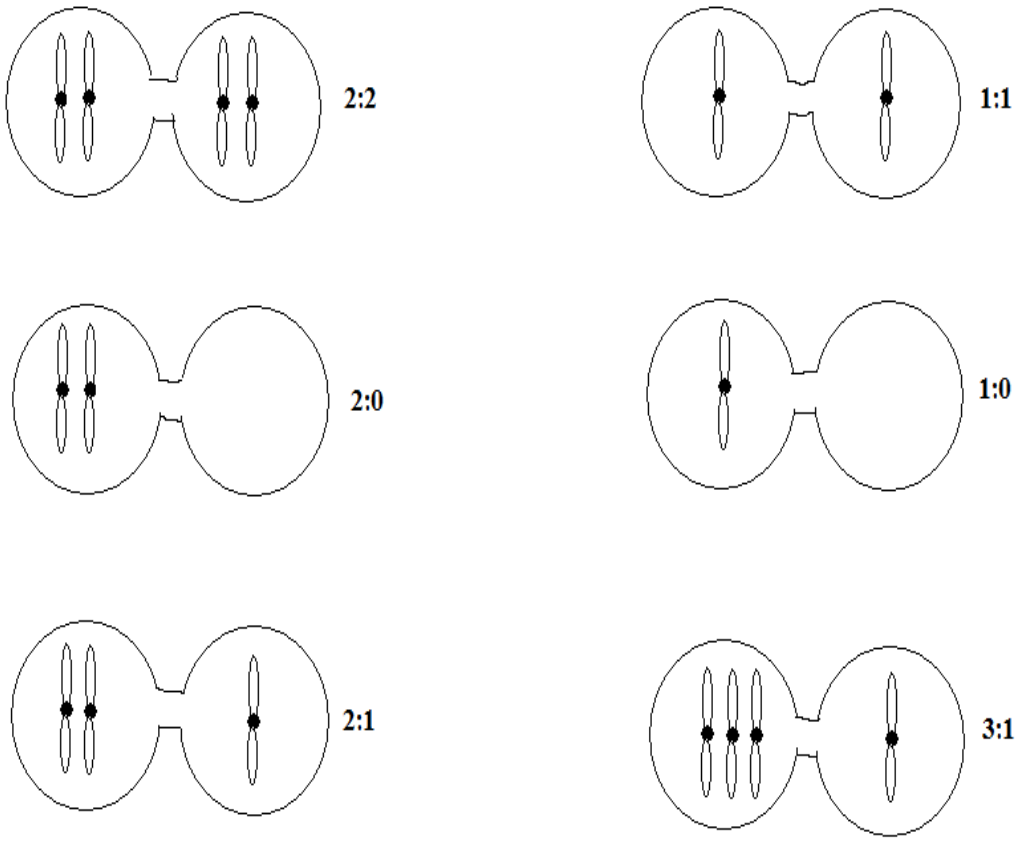

Figure 1. Chromosome Disjunction Ratios

NOTE: Schematic showing the different types of chromosomal disjunction.

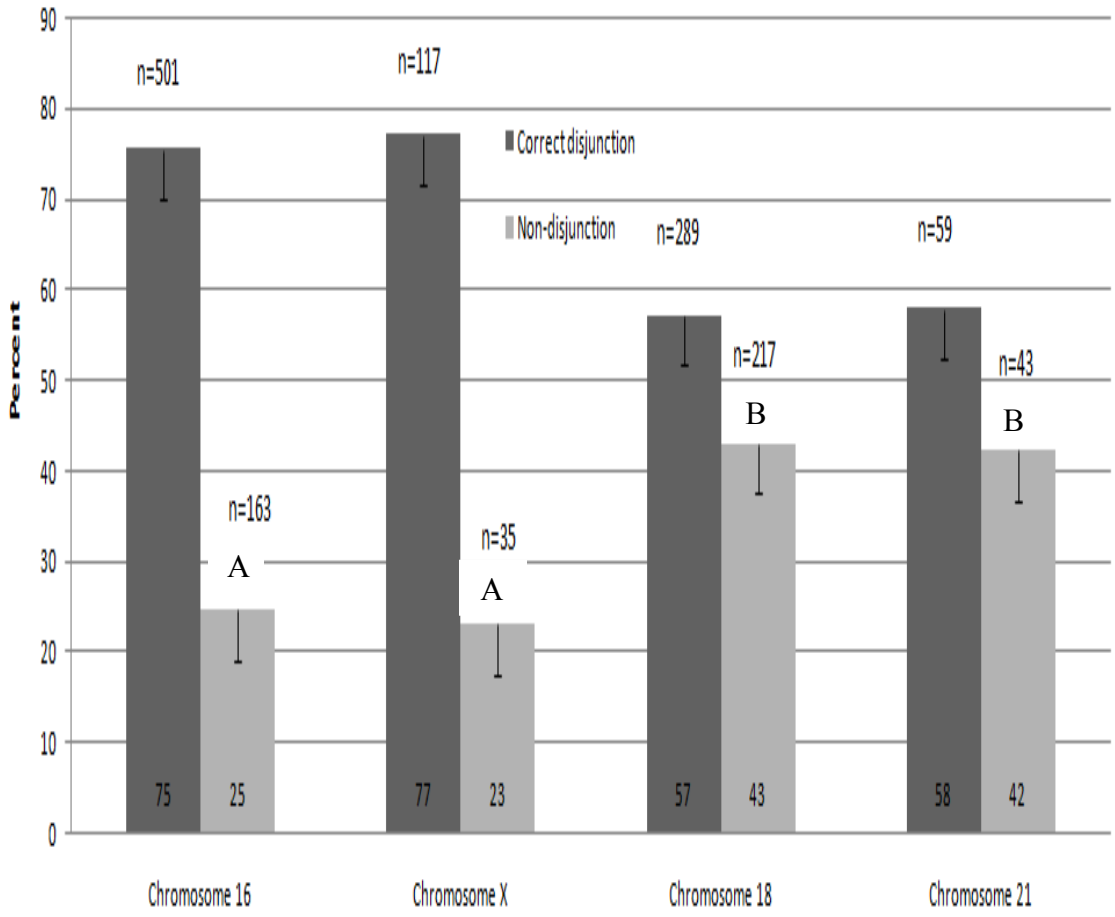

Figure 2. Intrinsic Frequency of Non-disjunction by Chromosome

NOTE: Graph comparing intrinsic rate of non-disjunction and correct distribution frequencies in chromosomes 16, 18, X, and 21. Differences in the intrinsic rate of non-disjunction with the same letter are not significantly different. Differences in the intrinsic rate of non-disjunction with different letters are significantly different at a 95% confidence interval. The standard error of the mean is represented by the error bars and the sample size (n) is indicated above each bar.

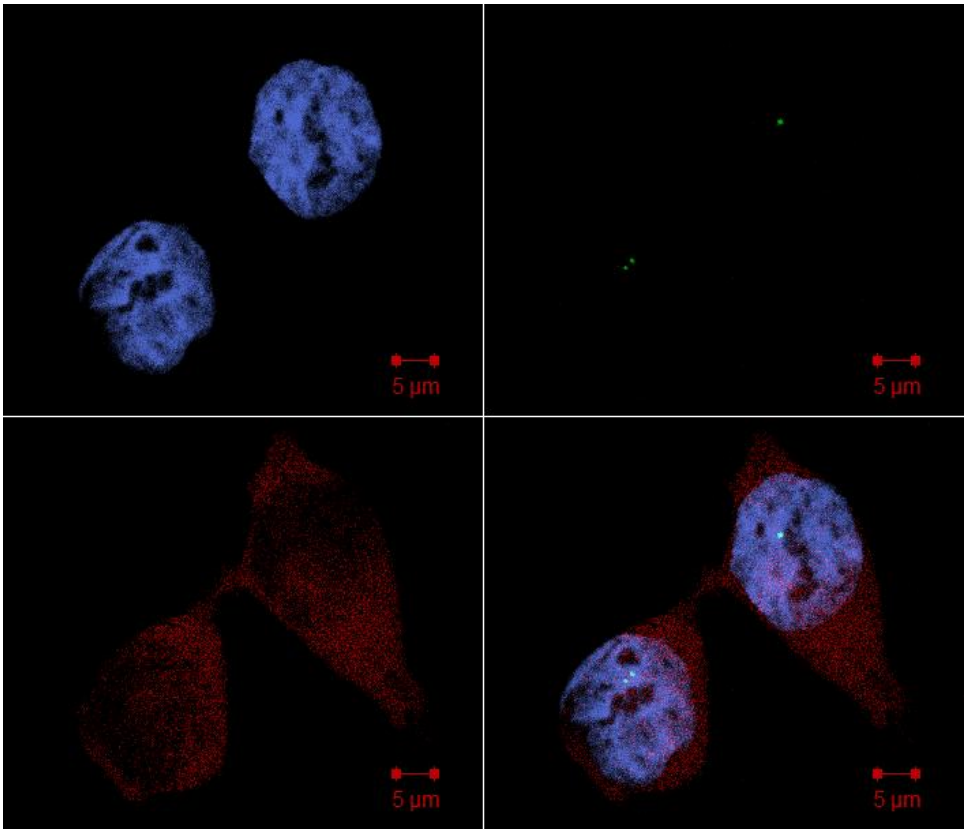

Figure 3. A micrograph of a fixed CHO-human hybrid cell line GM11979 showing non-disjunction in a daughter pair. DNA (upper left) is labeled with DAPI, chromosome 16 is label by *in situ* hybridization with SpectrumGreen probe to the 16q11.2 chromosome region (upper right), microtubules are labeled with anti-tubulin antibody (lower left), and composite image (lower right). Scale bar represents 5µm.

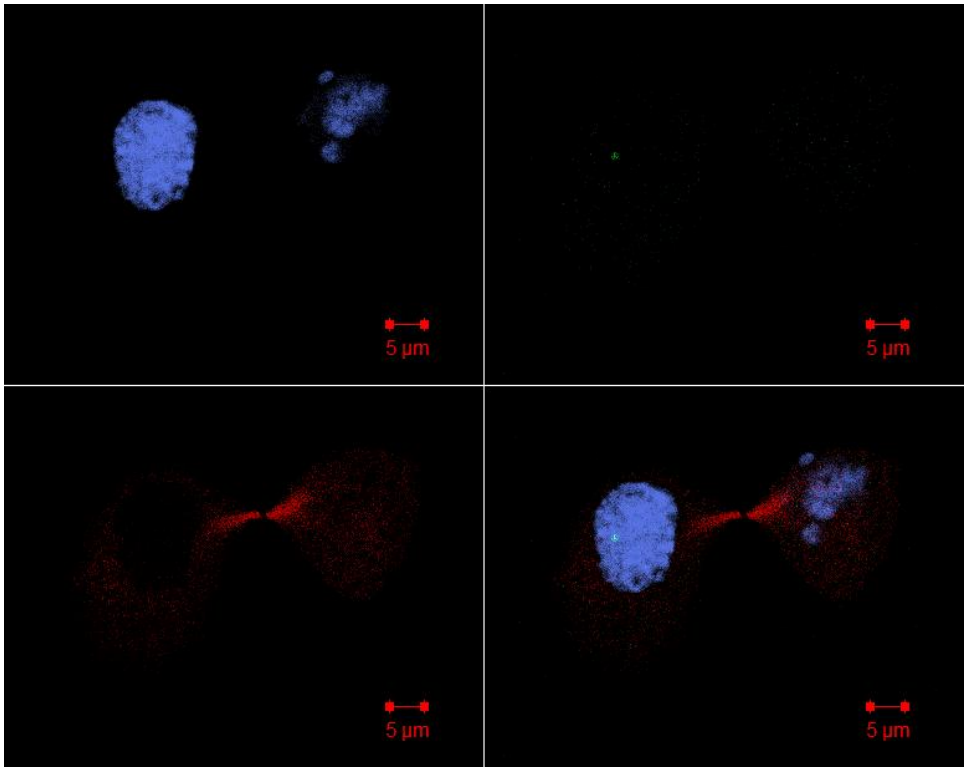

Figure 4. A micrograph of a fixed CHO-human hybrid cell line GM11979 showing non-disjunction in a daughter pair. DNA (upper left) is labeled with DAPI, chromosome 16 is label by *in situ* hybridization with SpectrumGreen probe to the 16q11.2 chromosome region (upper right), microtubules are labeled with anti-tubulin antibody (lower left), and composite image (lower right). Scale bar represents 5µm.

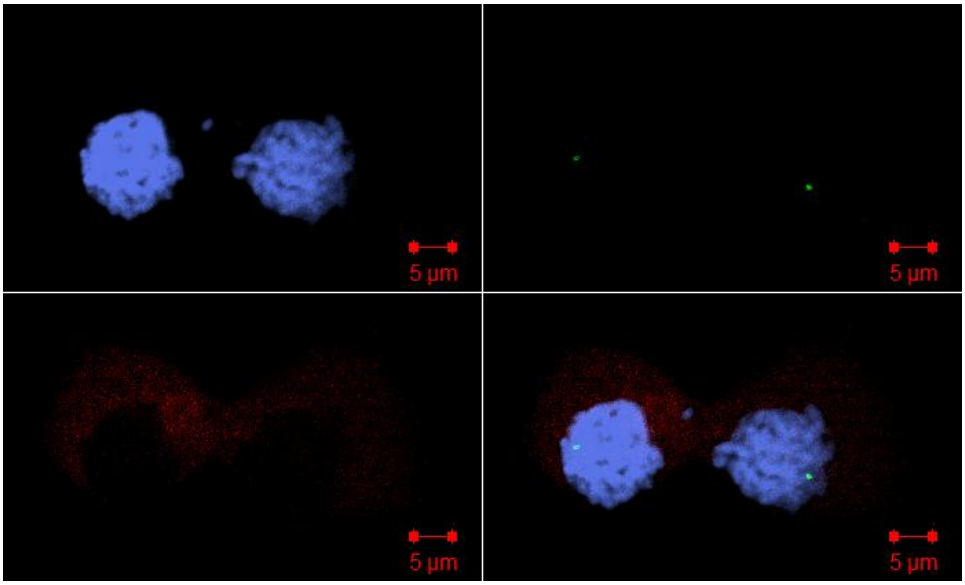

Figure 5. A micrograph of a fixed CHO-human hybrid cell line GM11979 showing correct segregation in a daughter pair. DNA (upper left) is labeled with DAPI, chromosome 16 is label by *in situ* hybridization with SpectrumGreen probe to the 16q11.2 chromosome region (upper right), microtubules are labeled with anti-tubulin antibody (lower left), and composite image (lower right). Scale bar represents 5µm.

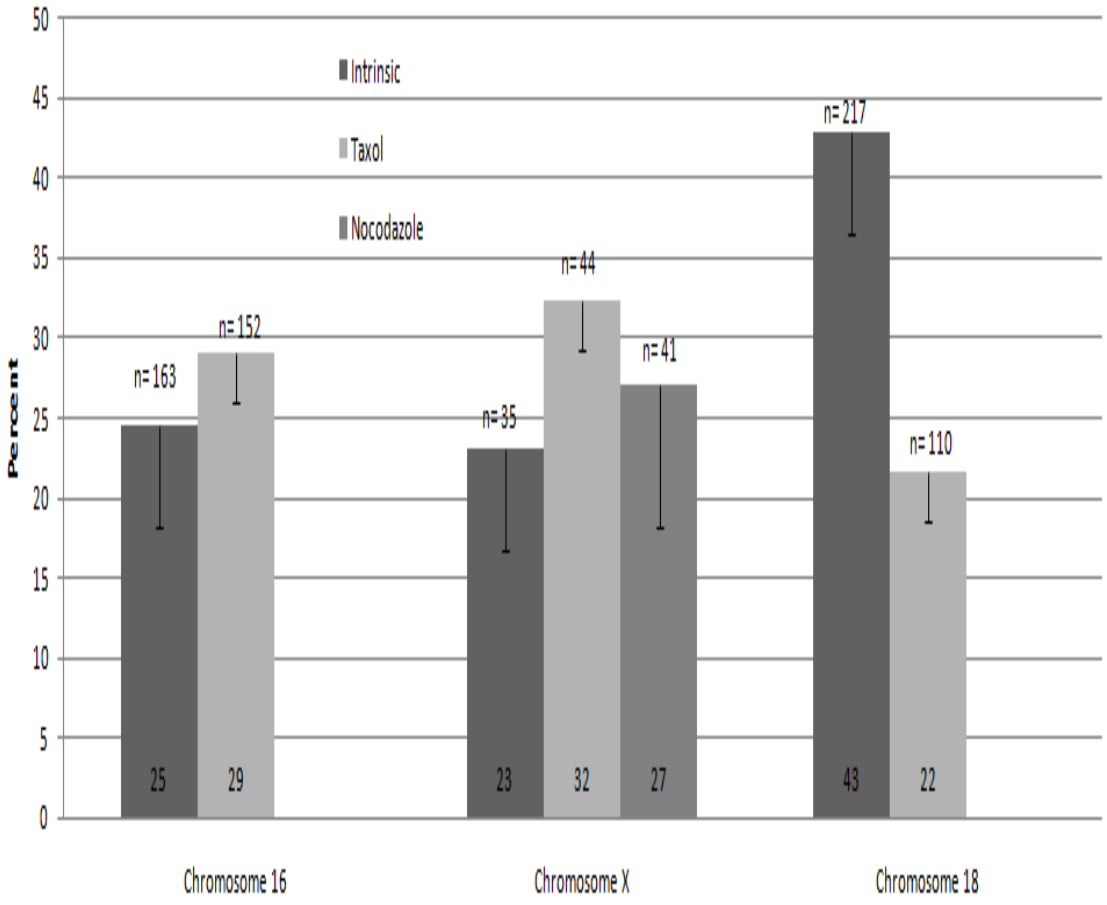

Figure 6. Effects of Microtubule Perturbation on Non-disjunction Frequencies

NOTE: Graph comparing non-disjunction and correct distribution in untreated and treated cells in chromosomes 16, 18 and X. The standard error of the mean is represented by the error bars and the sample size (n) is indicated above each bar.

Table 1. The Effects of Microtubule Perturbation on the Type of Disjunction in Chromosomes 16, X, 18, and 21

Chromosome/Treatment	1:1	2:2	3:3	4:4	1:0	2:0	2:1	3:0	3:1	3:2	4:0	4:1	4:2	4:3	5:1	Midbody	n= number of daughter pairs counted
Chromosome 16/Intrinsic	70.5%	5.0%	0.0%	0.0%	13.6%	4.5%	5.1%	0.0%	0.5%	0.0%	0.0%	0.8%	0.0%	0.0%	0.0%	0.2%	n= 664
Chromosome 16/Taxol	67.7%	3.3%	0.0%	0.0%	13.0%	6.1%	8.6%	0.6%	0.4%	0.4%	0.0%	0.0%	0.0%	0.0%	0.0%	0.0%	n= 523
Chromosome X/Intrinsic	59.2%	17.1%	0.7%	0.0%	3.9%	2.6%	11.2%	0.7%	3.3%	0.7%	0.0%	0.0%	0.7%	0.0%	0.0%	0.0%	n= 152
Chromosome X/Taxol	64.7%	2.9%	0.0%	0.0%	19.1%	5.9%	5.9%	0.7%	0.7%	0.0%	0.0%	0.0%	0.0%	0.0%	0.0%	0.0%	n= 136
Chromosome X/Nocodazole	63.6%	9.3%	1.3%	0.0%	9.9%	7.3%	7.3%	0.0%	2.6%	0.0%	0.0%	0.0%	0.0%	0.0%	0.0%	0.0%	n= 151
Chromosome 18/Intrinsic	22.3%	28.7%	4.7%	1.4%	18.6%	7.5%	10.9%	1.2%	1.6%	1.4%	0.2%	0.2%	0.4%	1.2%	0.0%	0.0%	n= 506
Chromosome 18/ Taxol	56.5%	19.9%	1.6%	0.4%	4.3%	5.1%	7.9%	0.2%	1.8%	2.0%	0.0%	0.0%	0.2%	0.0%	0.2%	0.0%	n= 508
Chromosome 21/Intrinsic	8.8%	23.5%	21.6%	3.9%	5.9%	4.9%	3.9%	0.0%	8.8%	11.8%	0.0%	0.0%	3.9%	5.9%	0.0%	1.0%	n= 102

NOTE: Table showing the different types of distribution in untreated cells and treated-cells of Chromosomes 16, X, 18, 21.

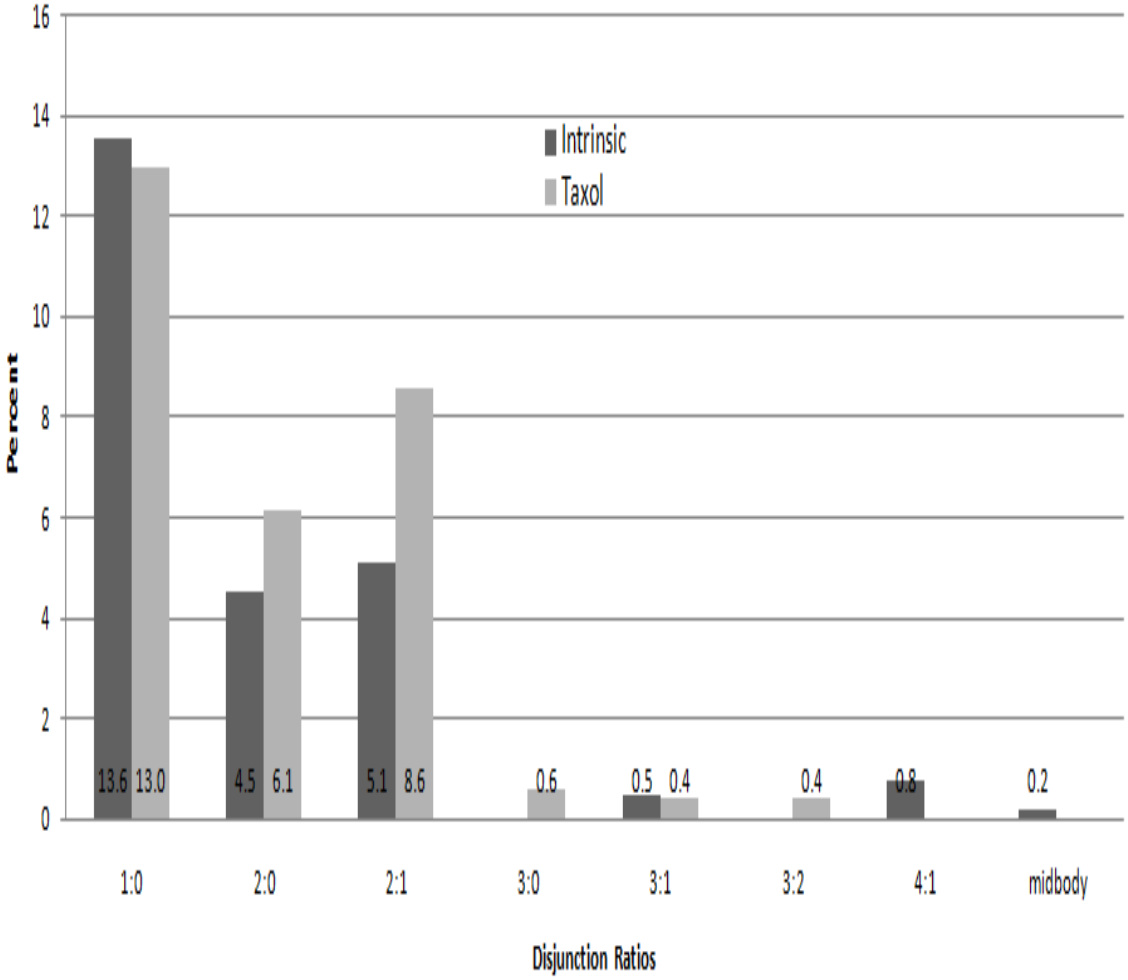

Figure 7. Effects of Microtubule Perturbation on Non-disjunction of Chromosome 16

NOTE: Graph comparing the non-disjunction ratios of chromosome 16 in untreated (intrinsic) cells and taxol-treated cells.

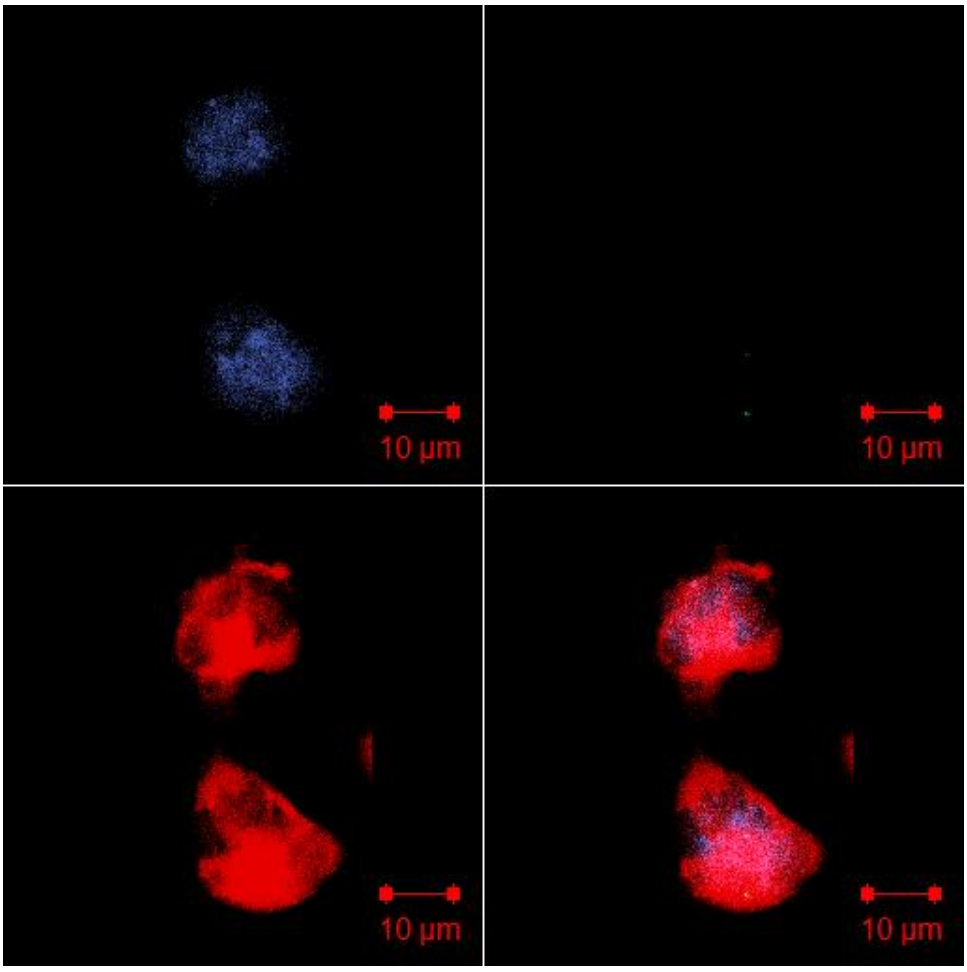

Figure 8. A micrograph of a fixed CHO-human hybrid cell line GM11979 treated with taxol showing non-disjunction in a daughter pair. DNA (upper left) is labeled with DAPI, chromosome 16 is label by *in situ* hybridization with SpectrumGreen probe to the 16q11.2 chromosome region (upper right), microtubules are labeled with anti-tubulin antibody (lower left), and composite image (lower right). Scale bar represents 10µm.

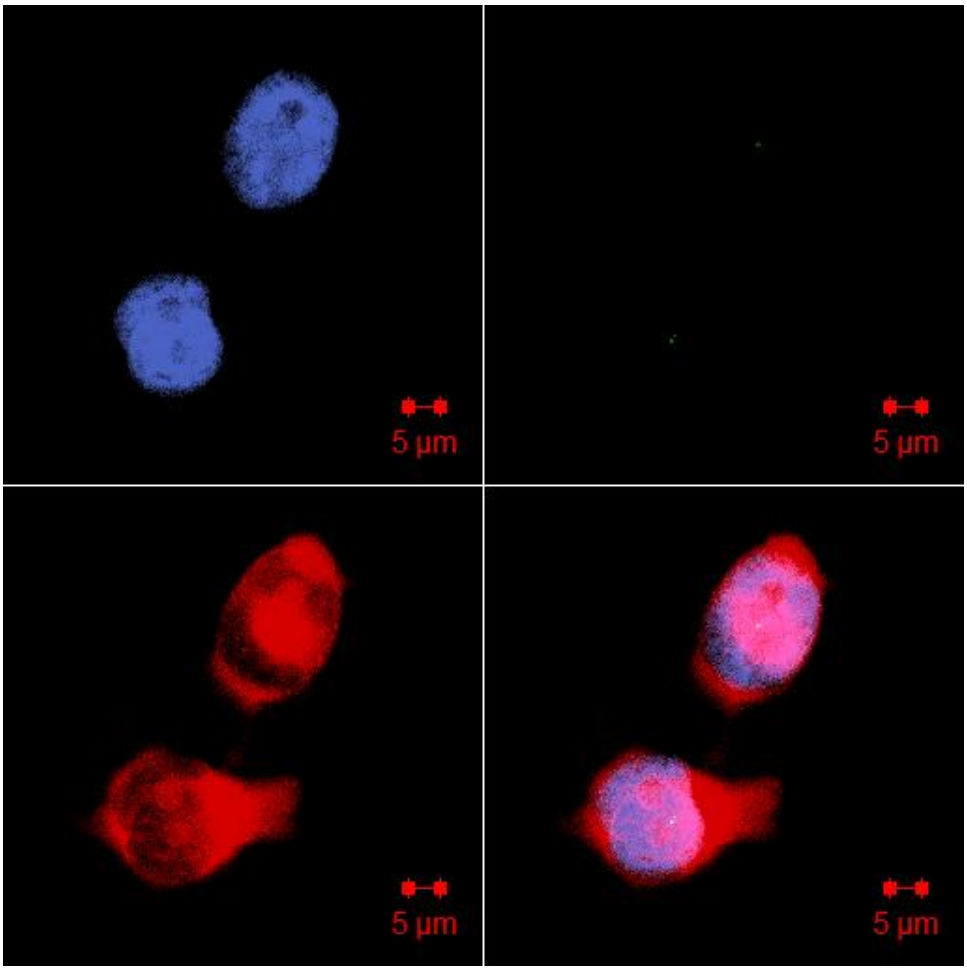

Figure 9. A micrograph of a fixed CHO-human hybrid cell line GM11979 treated with taxol showing non-disjunction in a daughter pair. DNA (upper left) is labeled with DAPI, chromosome 16 is label by *in situ* hybridization with SpectrumGreen probe to the 16q11.2 chromosome region (upper right), microtubules are labeled with anti-tubulin antibody (lower left), and composite image (lower right). Scale bar represents 5µm.

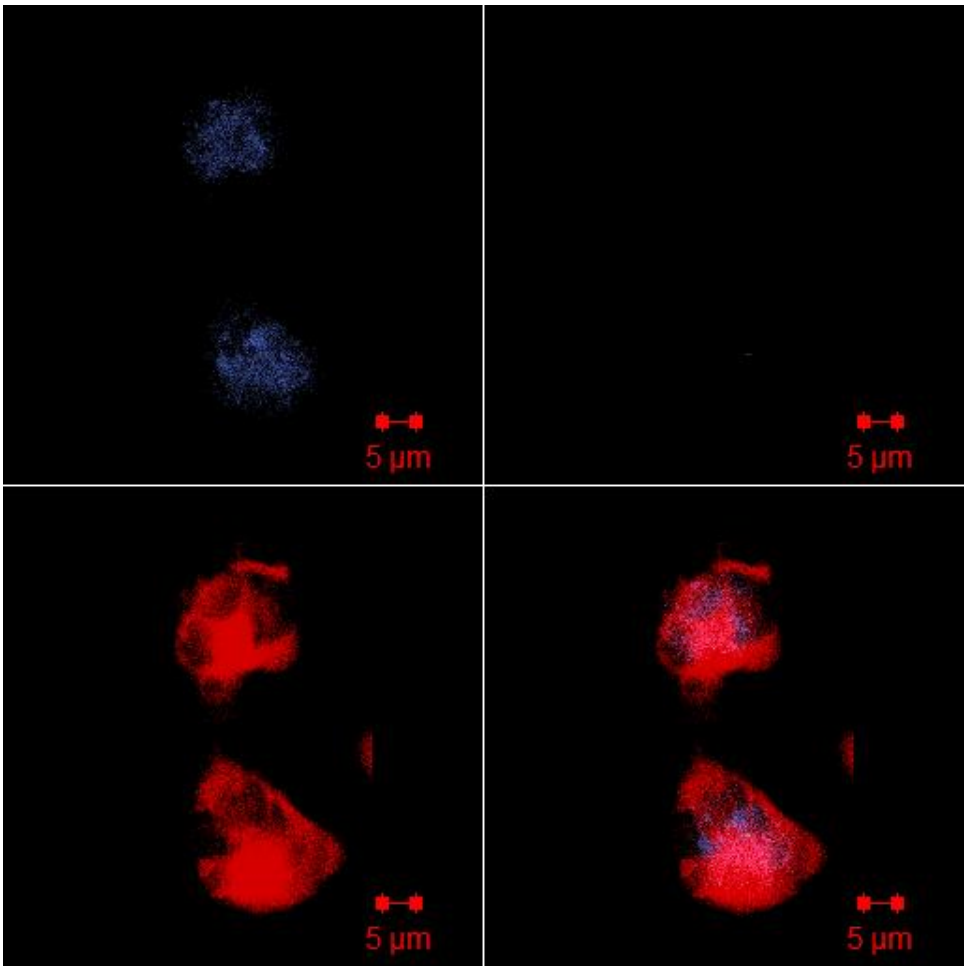

Figure 10. A micrograph of a fixed CHO-human hybrid cell line GM11979 treated with taxol showing non-disjunction in a daughter pair. DNA (upper left) is labeled with DAPI, chromosome 16 is label by *in situ* hybridization with SpectrumGreen probe to the 16q11.2 chromosome region (upper right), microtubules are labeled with anti-tubulin antibody (lower left), and composite image (lower right). Scale bar represents 5µm.

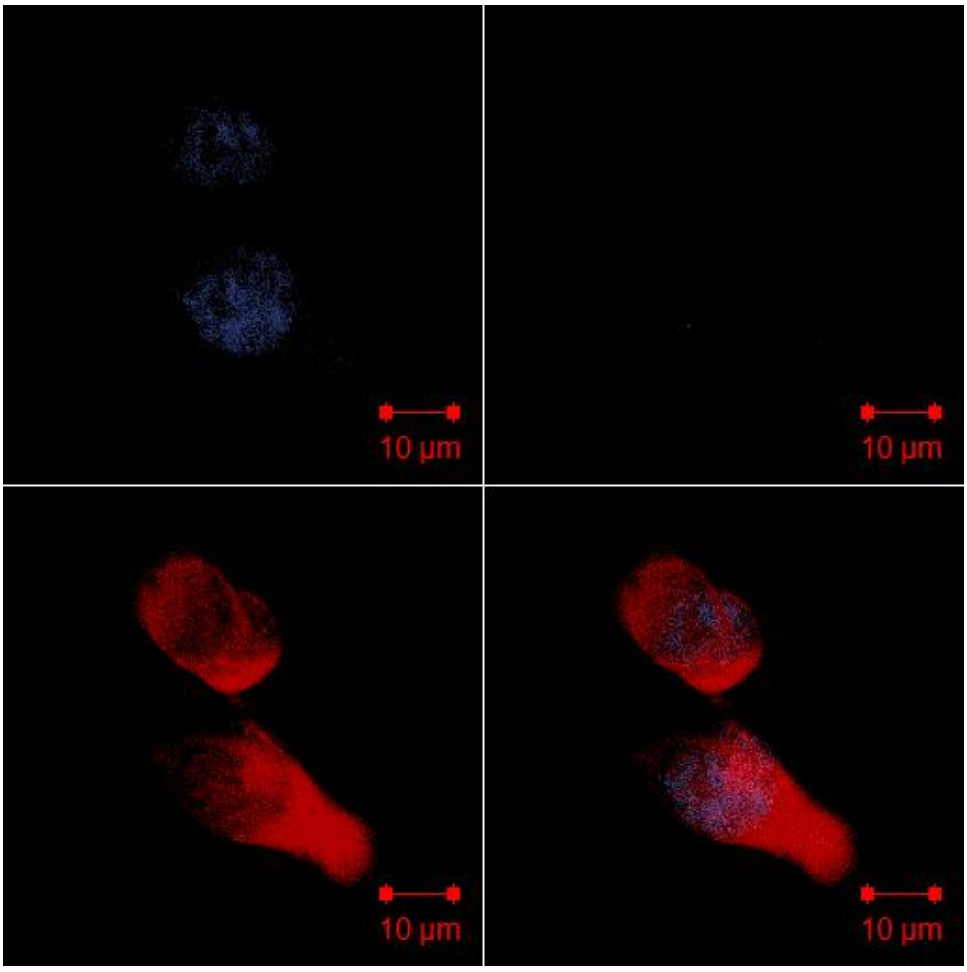

Figure 11. A micrograph of a fixed CHO-human hybrid cell line GM11979 treated with taxol showing non-disjunction in a daughter pair. DNA (upper left) is labeled with DAPI, chromosome 16 is label by *in situ* hybridization with SpectrumGreen probe to the 16q11.2 chromosome region (upper right), microtubules are labeled with anti-tubulin antibody (lower left), and composite image (lower right). Scale bar represents 10µm.

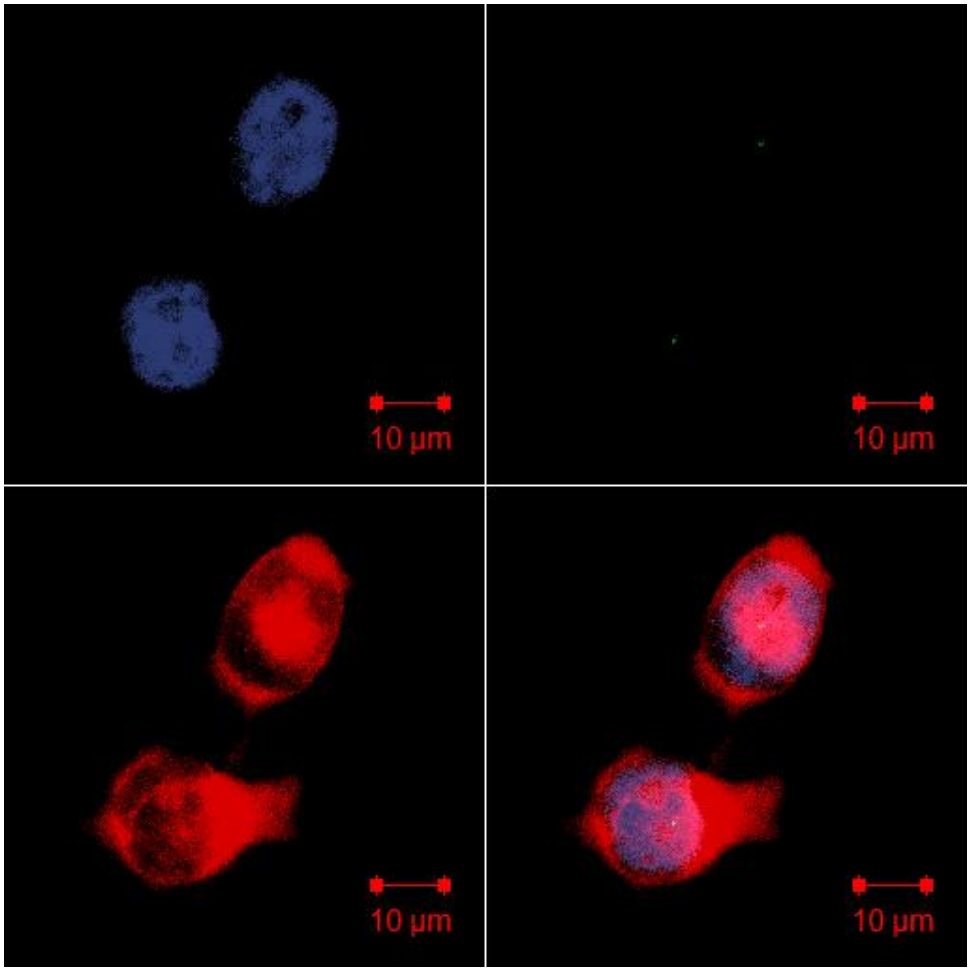

Figure 12. A micrograph of a fixed CHO-human hybrid cell line GM11979 treated with taxol showing correct segregation in a daughter pair. DNA (upper left) is labeled with DAPI, chromosome 16 is label by *in situ* hybridization with SpectrumGreen probe to the 16q11.2 chromosome region (upper right), microtubules are labeled with anti-tubulin antibody (lower left), and composite image (lower right). Scale bar represents 10µm.

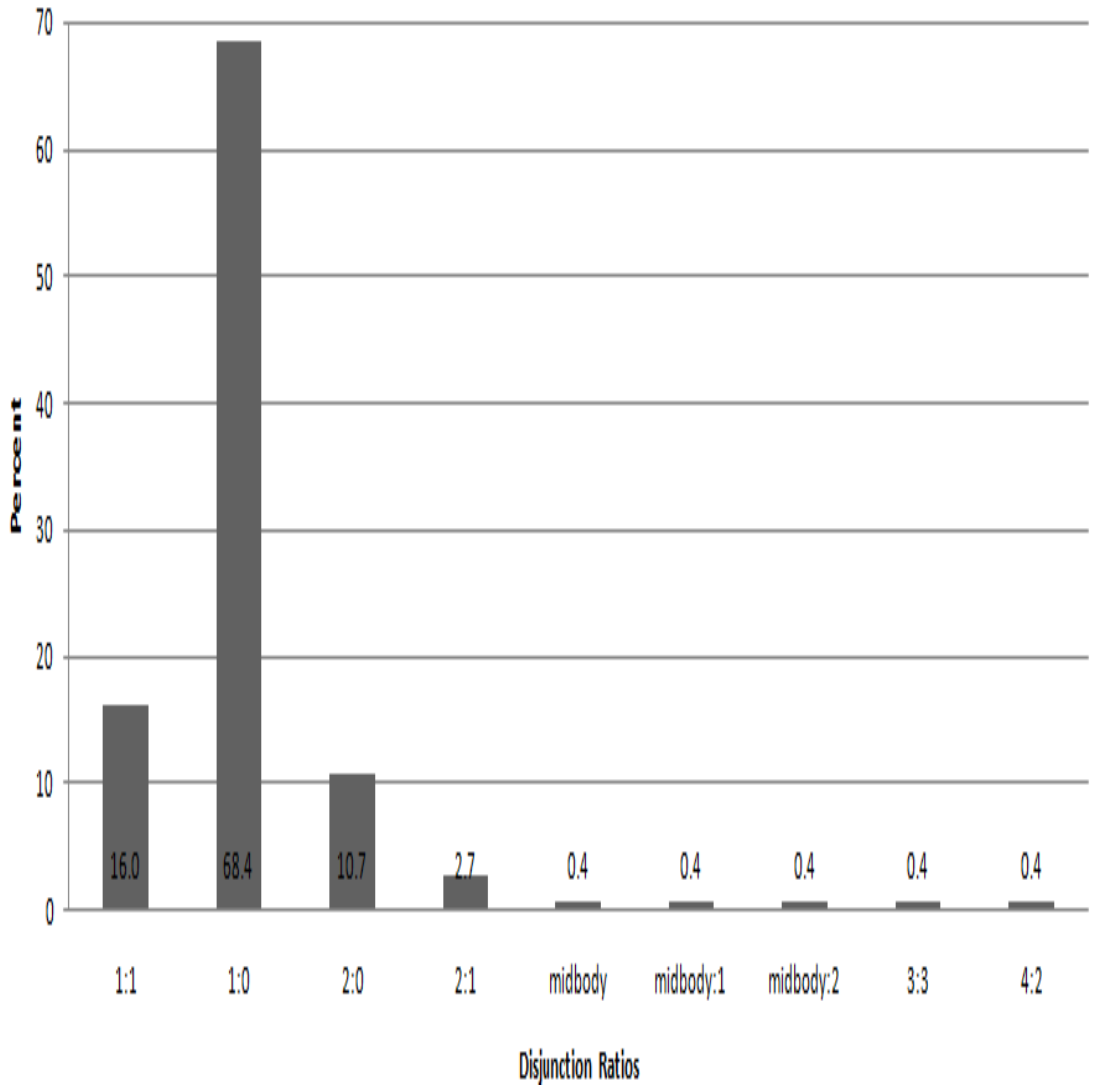

Figure 13. Chromosome 16 MUG Disjunction Ratios

NOTE: Graph comparing the distribution ratios in MUG cells probed for chromosome 16.

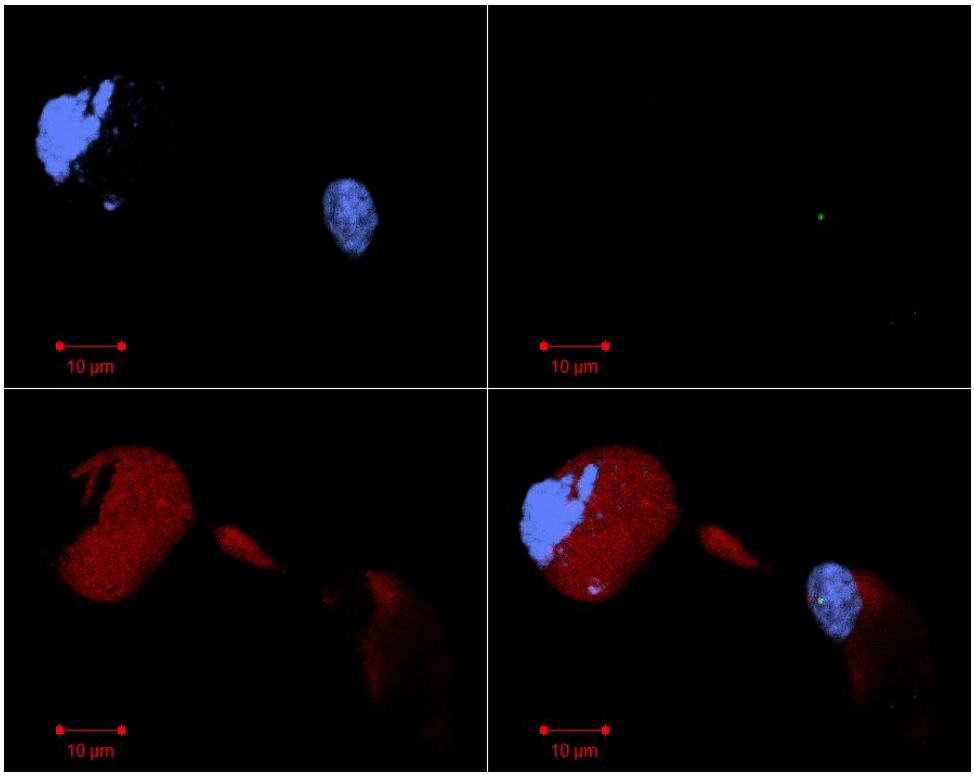

Figure 14. A micrograph of a fixed CHO-human hybrid cell line GM11979 treated with the MUG technique showing correct segregation in a daughter pair. DNA (upper left) is labeled with DAPI, chromosome 16 is label by *in situ* hybridization with SpectrumGreen probe to the 16q11.2 chromosome region (upper right), microtubules are labeled with anti-tubulin antibody (lower left), and composite image (lower right). Scale bar represents 10µm.

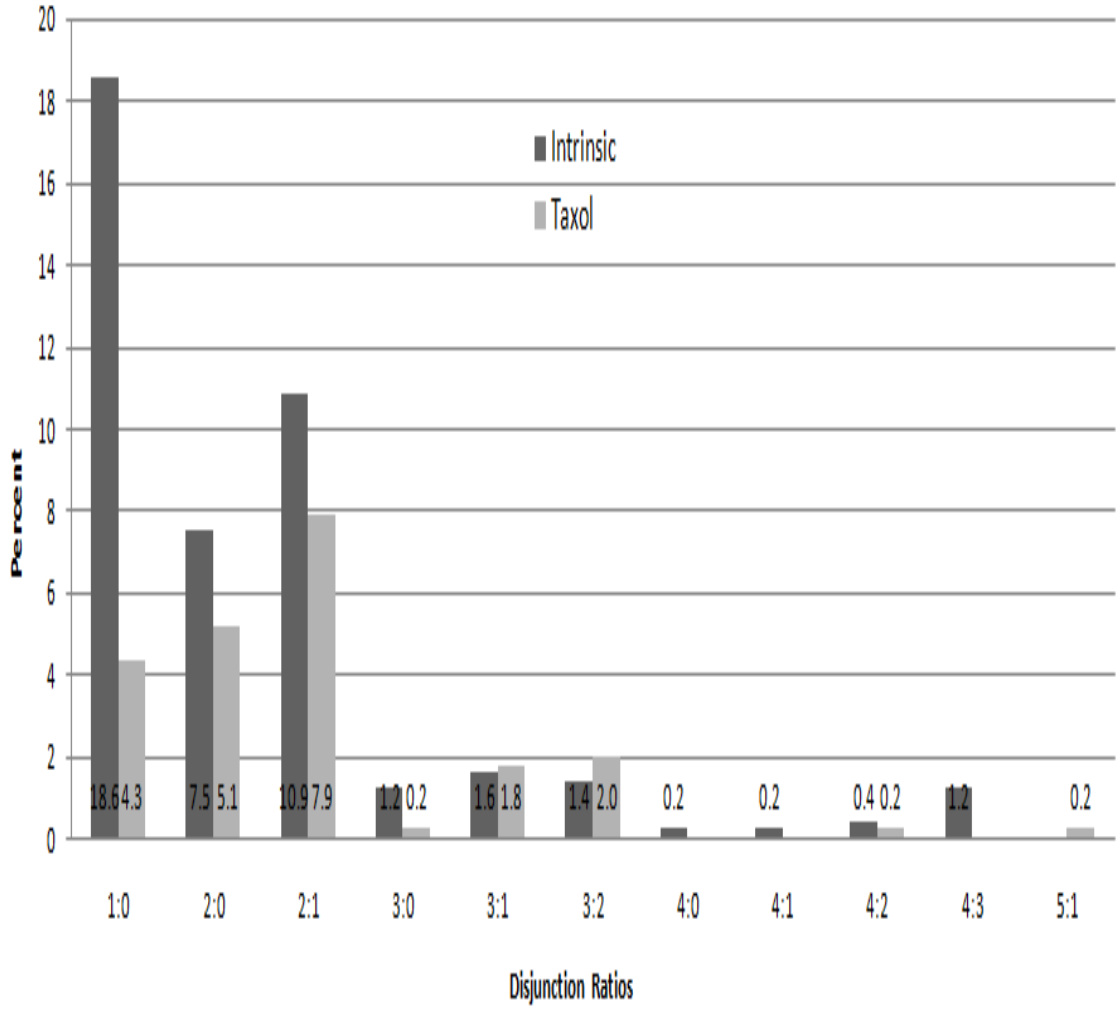

Figure 15. Effects of Microtubule Perturbation on Non-disjunction of Chromosome 18

NOTE: Graph comparing the non-disjunction ratios of chromosome 18 in untreated (intrinsic) cells and taxol-treated cells.

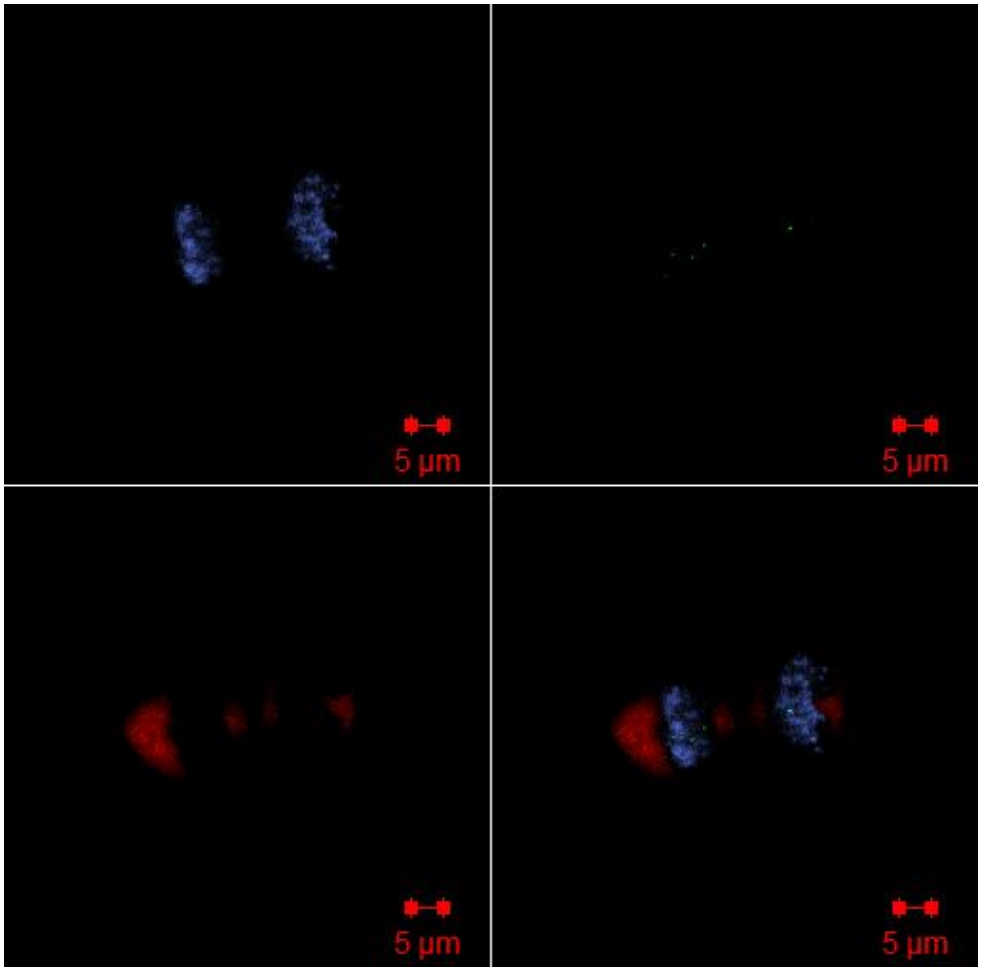

Figure 16. A micrograph of a fixed CHO-human hybrid cell line GM11130 showing non-disjunction in a daughter pair. DNA (upper left) is labeled with DAPI, chromosome 18 is label by *in situ* hybridization with green fluorophore probe to the 18p11.1-q11.1 chromosome region (upper right), microtubules are labeled with anti-tubulin antibody (lower left), and composite image (lower right). Scale bar represents 5µm.

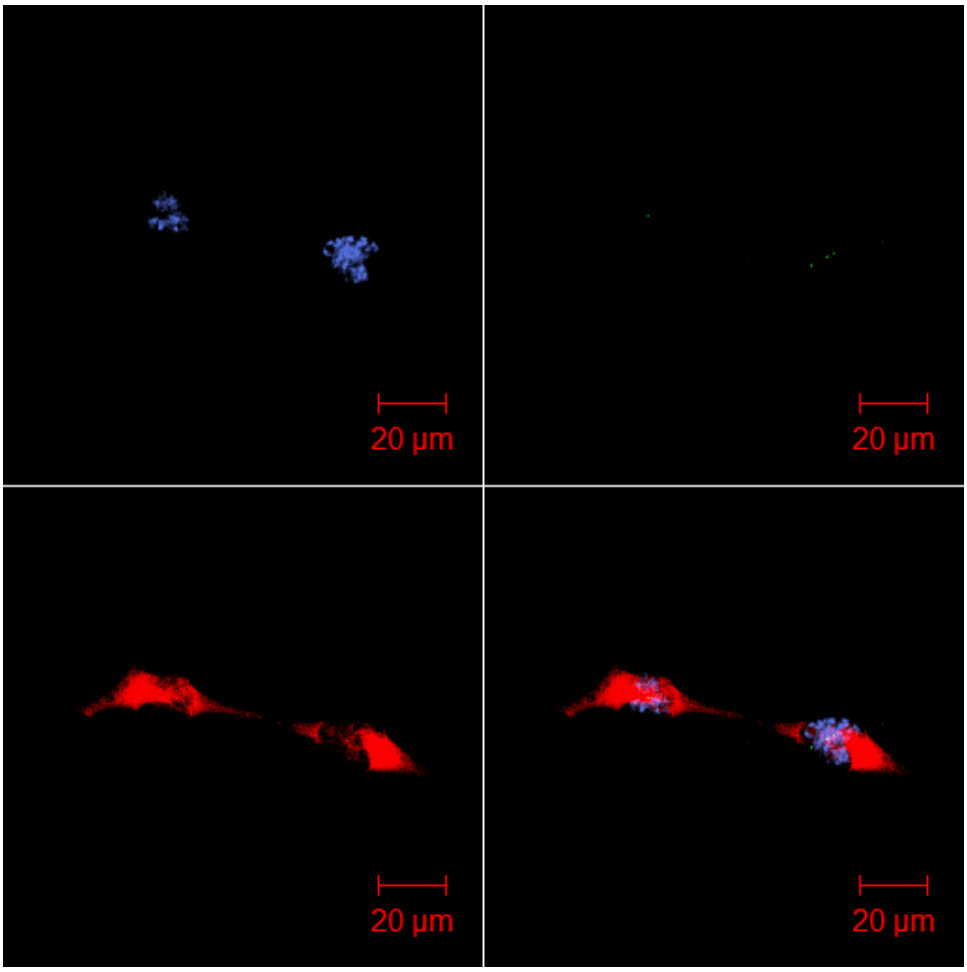

Figure 17. A micrograph of a fixed CHO-human hybrid cell line GM11130 showing non-disjunction in a daughter pair. DNA (upper left) is labeled with DAPI, chromosome 18 is label by *in situ* hybridization with green fluorophore probe to the 18p11.1-q11.1 chromosome region (upper right), microtubules are labeled with anti-tubulin antibody (lower left), and composite image (lower right). Scale bar represents 20µm.

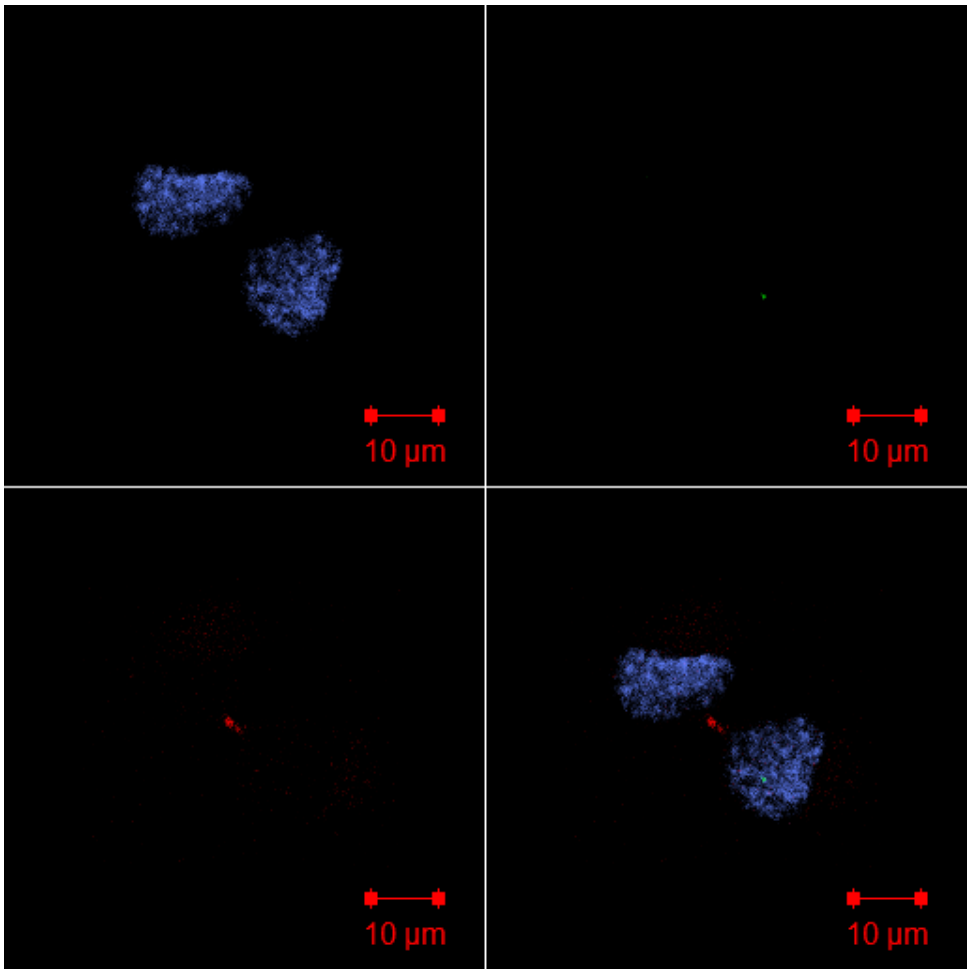

Figure 18. A micrograph of a fixed CHO-human hybrid cell line GM11130 showing non-disjunction in a daughter pair. DNA (upper left) is labeled with DAPI, chromosome 18 is label by *in situ* hybridization with green fluorophore probe to the 18p11.1-q11.1 chromosome region (upper right), microtubules are labeled with anti-tubulin antibody (lower left), and composite image (lower right). Scale bar represents 10µm.

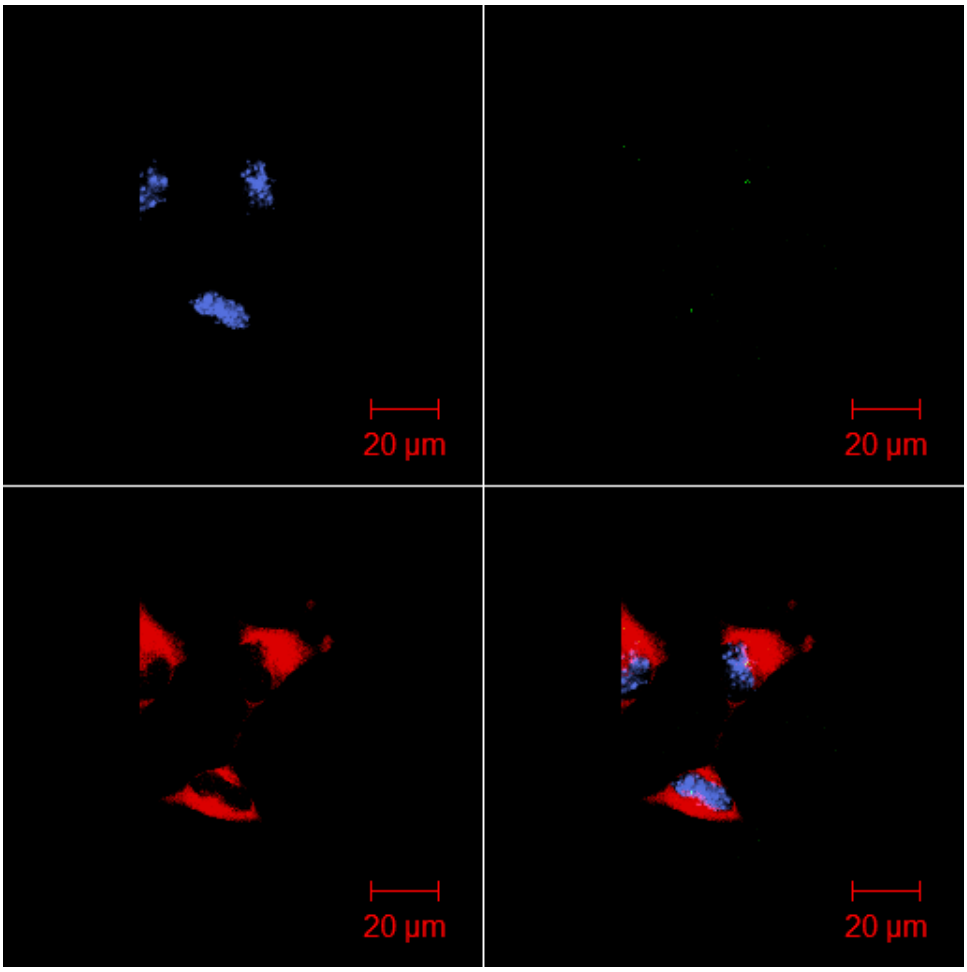

Figure 19. A micrograph of a fixed CHO-human hybrid cell line GM11130 showing correct segregation in a daughter pair. DNA (upper left) is labeled with DAPI, chromosome 18 is label by *in situ* hybridization with green fluorophore probe to the 18p11.1-q11.1 chromosome region (upper right), microtubules are labeled with anti-tubulin antibody (lower left), and composite image (lower right). Scale bar represents 20µm.

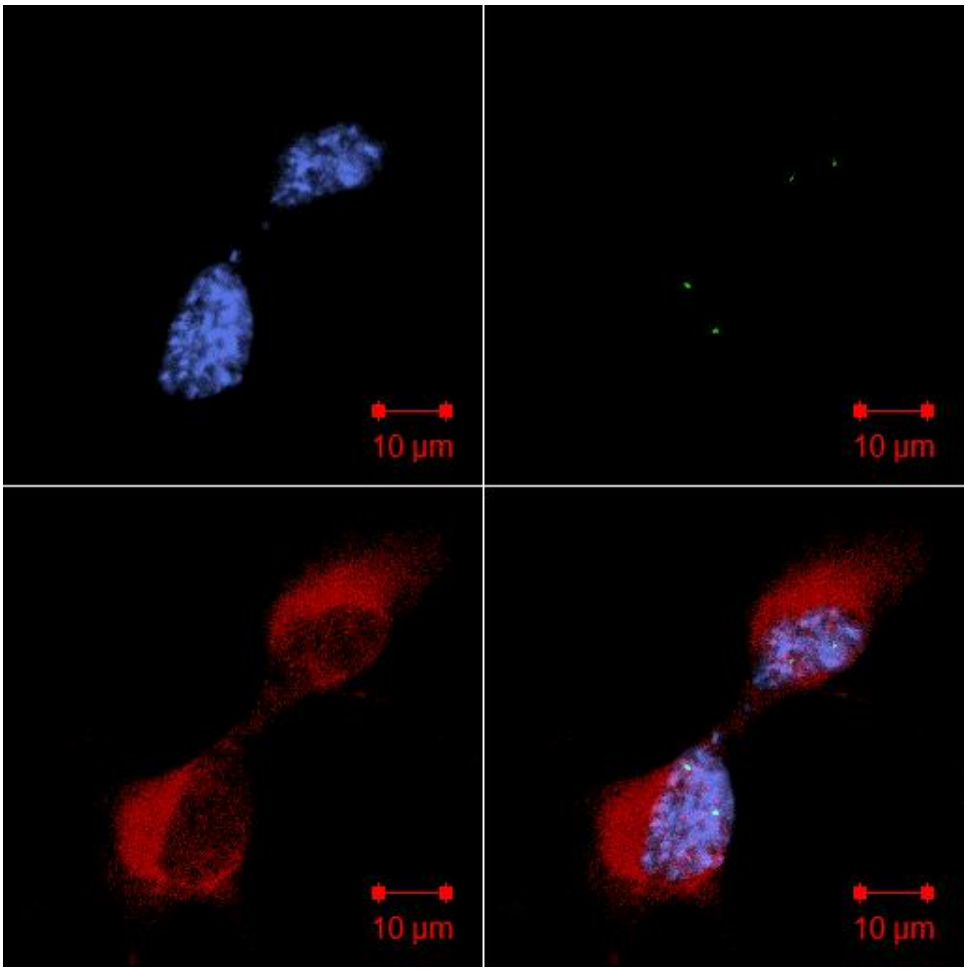

Figure 20. A micrograph of a fixed CHO-human hybrid cell line GM11130 showing correct segregation in a daughter pair. DNA (upper left) is labeled with DAPI, chromosome 18 is label by *in situ* hybridization with green fluorophore probe to the 18p11.1-q11.1 chromosome region (upper right), microtubules are labeled with anti-tubulin antibody (lower left), and composite image (lower right). Scale bar represents 10µm.

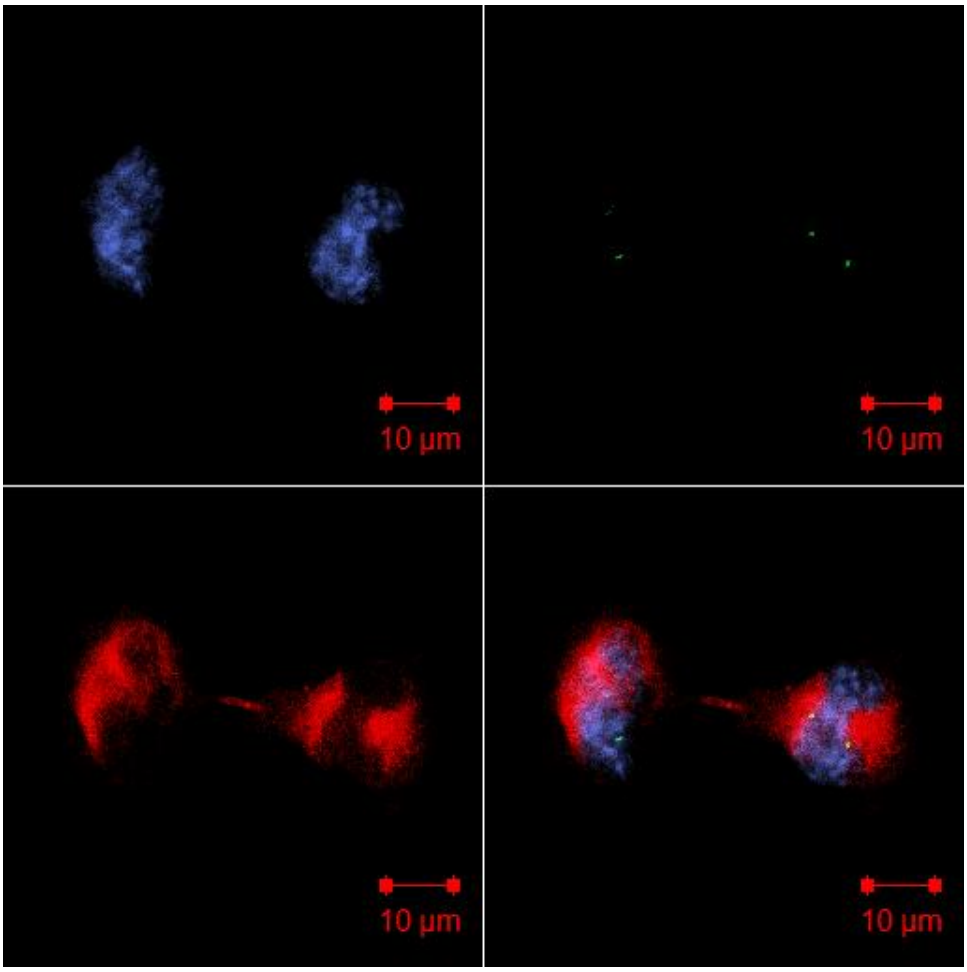

Figure 21. A micrograph of a fixed CHO-human hybrid cell line GM11130 showing correct segregation in a daughter pair. DNA (upper left) is labeled with DAPI, chromosome 18 is label by *in situ* hybridization with green fluorophore probe to the 18p11.1-q11.1 chromosome region (upper right), microtubules are labeled with anti-tubulin antibody (lower left), and composite image (lower right). Scale bar represents 10µm.

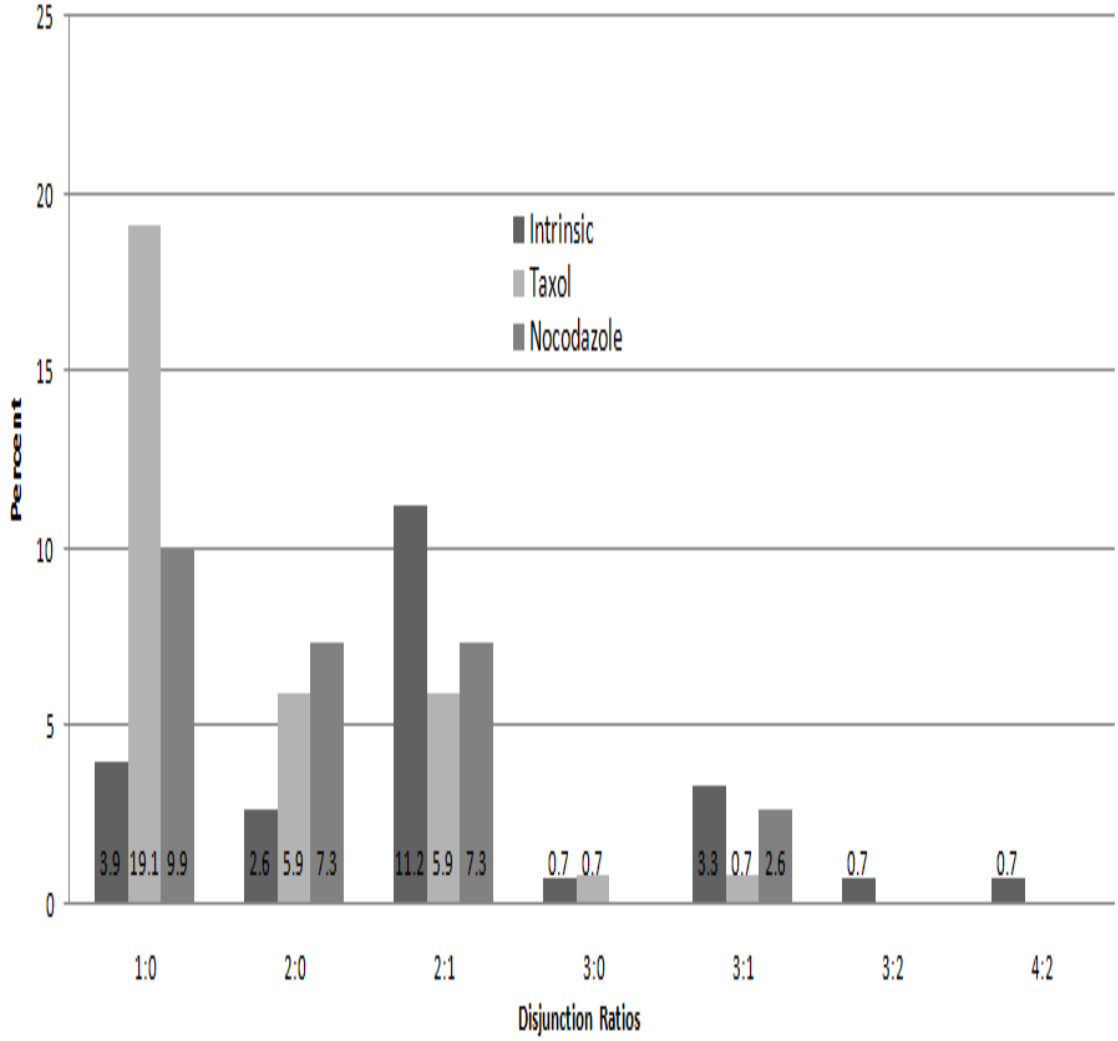

Figure 22. Effects of Microtubule Perturbation on Non-disjunction of Chromosome X

NOTE: Graph comparing the non-disjunction ratios of chromosome X in untreated (intrinsic) cells, taxol-treated cells and nocodazole-treated cells.

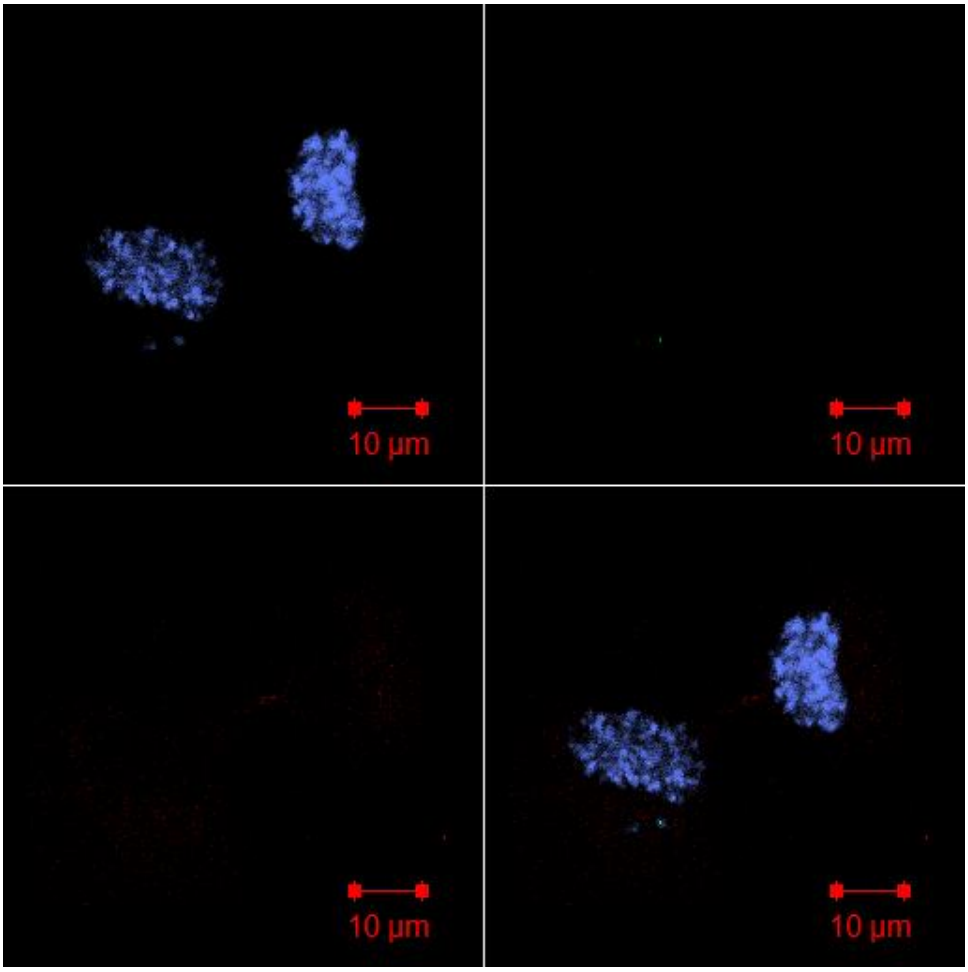

Figure 23. A micrograph of a fixed CHO-human hybrid cell line GM11130 showing non-disjunction in a daughter pair. DNA (upper left) is labeled with DAPI, chromosome X is label by *in situ* hybridization with green fluorophore probe to the Xp11.1-q11.1 chromosome region (upper right), microtubules are labeled with anti-tubulin antibody (lower left), and composite image (lower right). Scale bar represents 10µm.

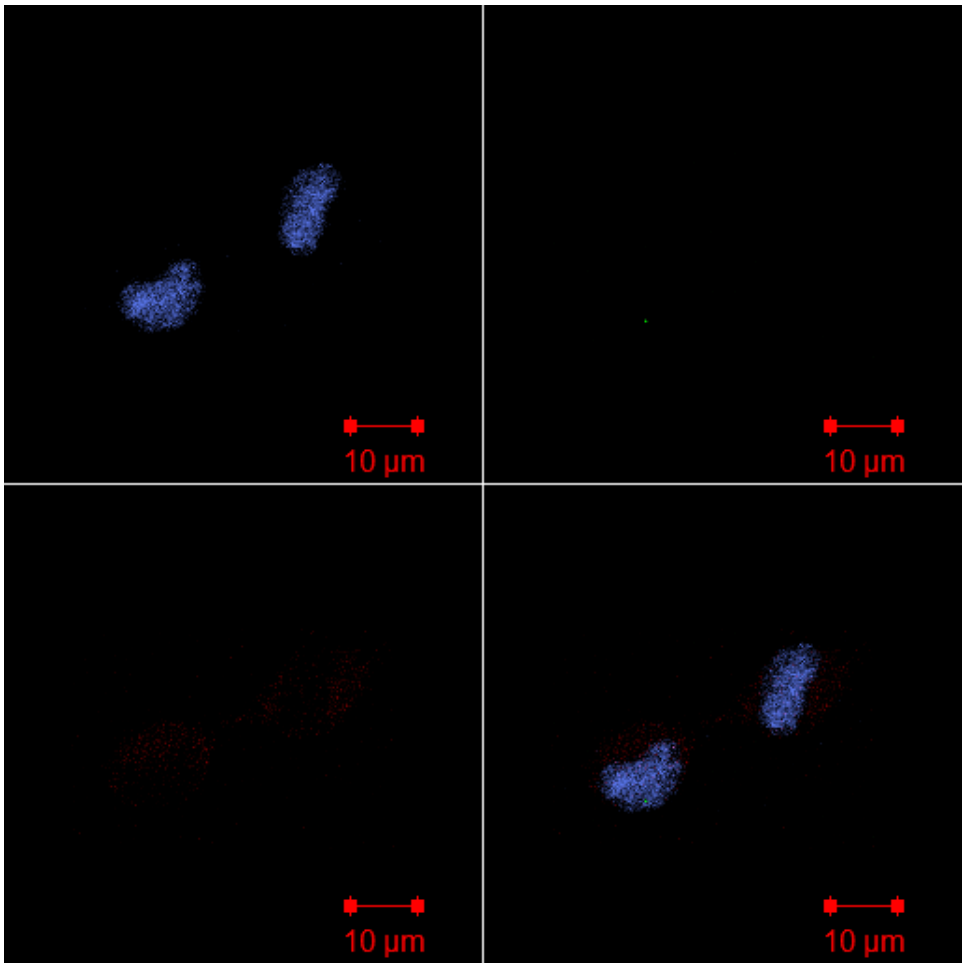

Figure 24. A micrograph of a fixed CHO-human hybrid cell line GM11130 treated with taxol showing non-disjunction in a daughter pair. DNA (upper left) is labeled with DAPI, chromosome X is label by *in situ* hybridization with SpectrumGreen probe to the Xp11.1-q11.1 chromosome region (upper right), microtubules are labeled with anti-tubulin antibody (lower left), and composite image (lower right). Scale bar represents 10µm.

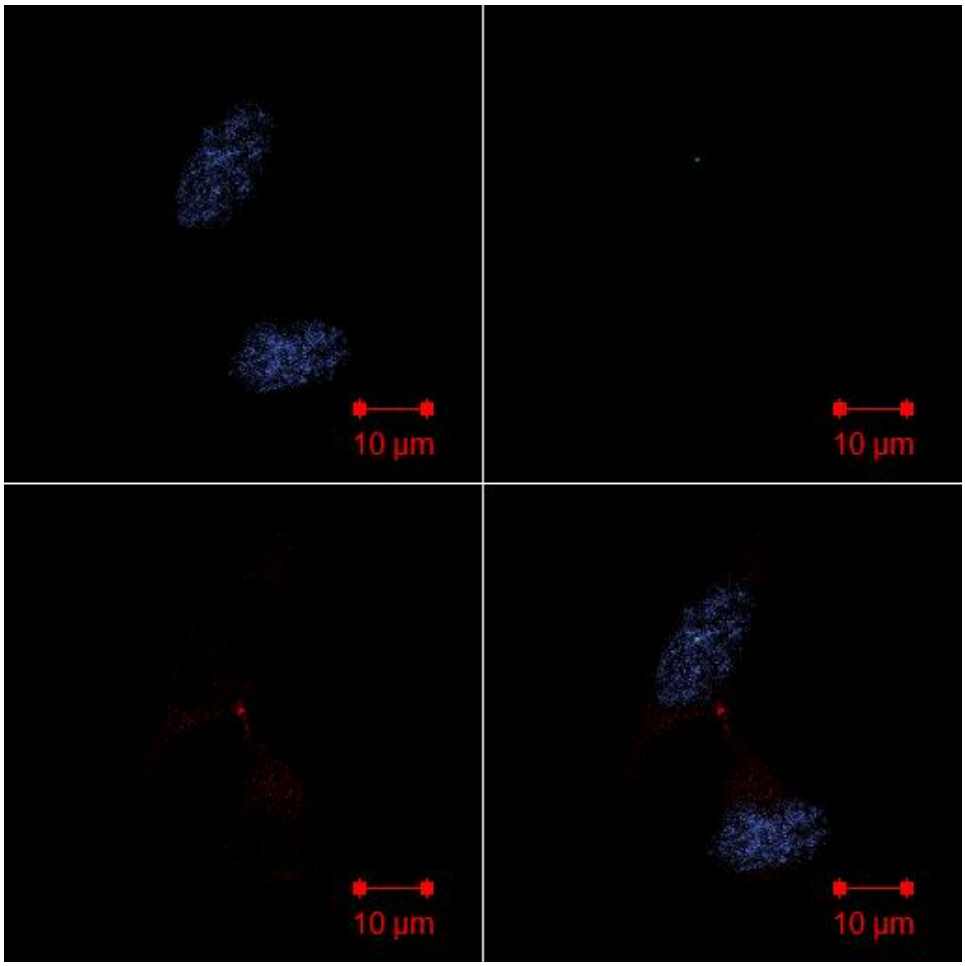

Figure 25. A micrograph of a fixed CHO-human hybrid cell line GM11130 treated with taxol showing non-disjunction in a daughter pair. DNA (upper left) is labeled with DAPI, chromosome X is label by *in situ* hybridization with SpectrumGreen probe to the Xp11.1-q11.1 chromosome region (upper right), microtubules are labeled with anti-tubulin antibody (lower left), and composite image (lower right). Scale bar represents 10µm.

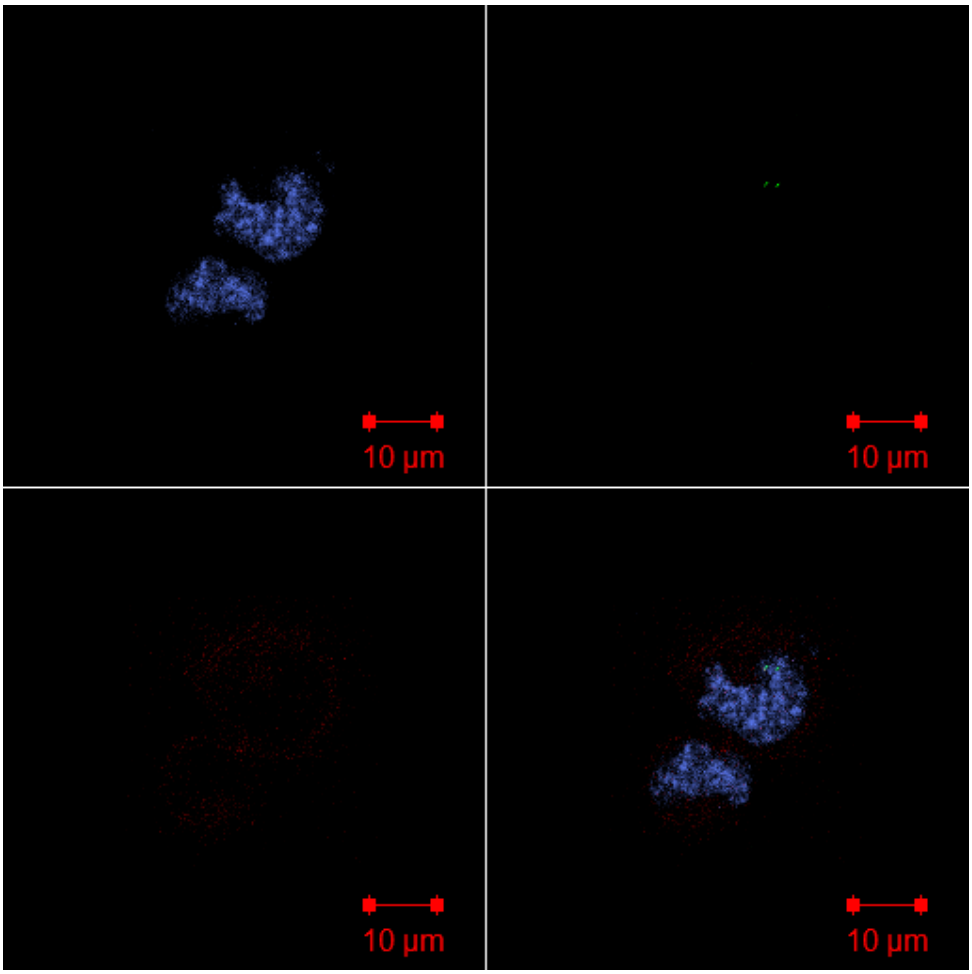

Figure 26. A micrograph of a fixed CHO-human hybrid cell line GM11130 treated with nocodazole showing non-disjunction in a daughter pair. DNA (upper left) is labeled with DAPI, chromosome X is label by *in situ* hybridization with SpectrumGreen probe to the Xp11.1-q11.1 chromosome region (upper right), microtubules are labeled with anti-tubulin antibody (lower left), and composite image (lower right). Scale bar represents 10µm.

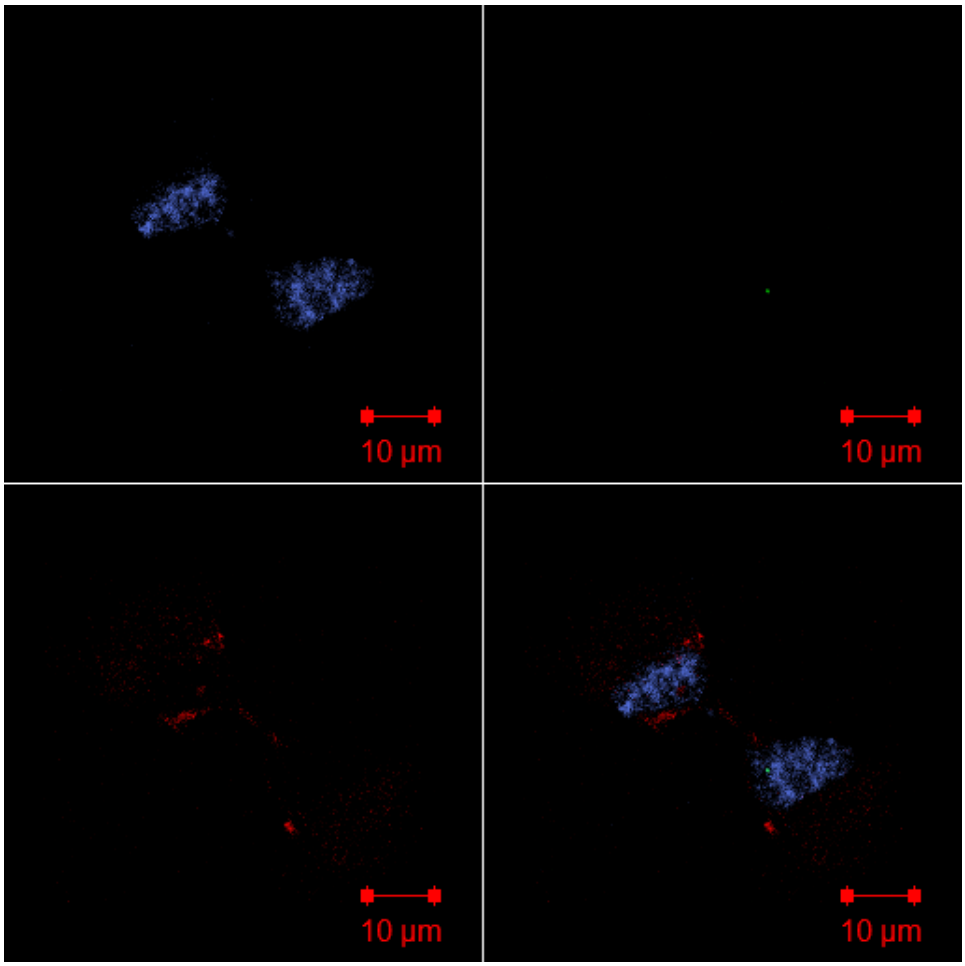

Figure 27. A micrograph of a fixed CHO-human hybrid cell line GM11130 treated with nocodazole showing non-disjunction in a daughter pair. DNA (upper left) is labeled with DAPI, chromosome X is label by *in situ* hybridization with SpectrumGreen probe to the Xp11.1-q11.1 chromosome region (upper right), microtubules are labeled with anti-tubulin antibody (lower left), and composite image (lower right). Scale bar represents 10µm.

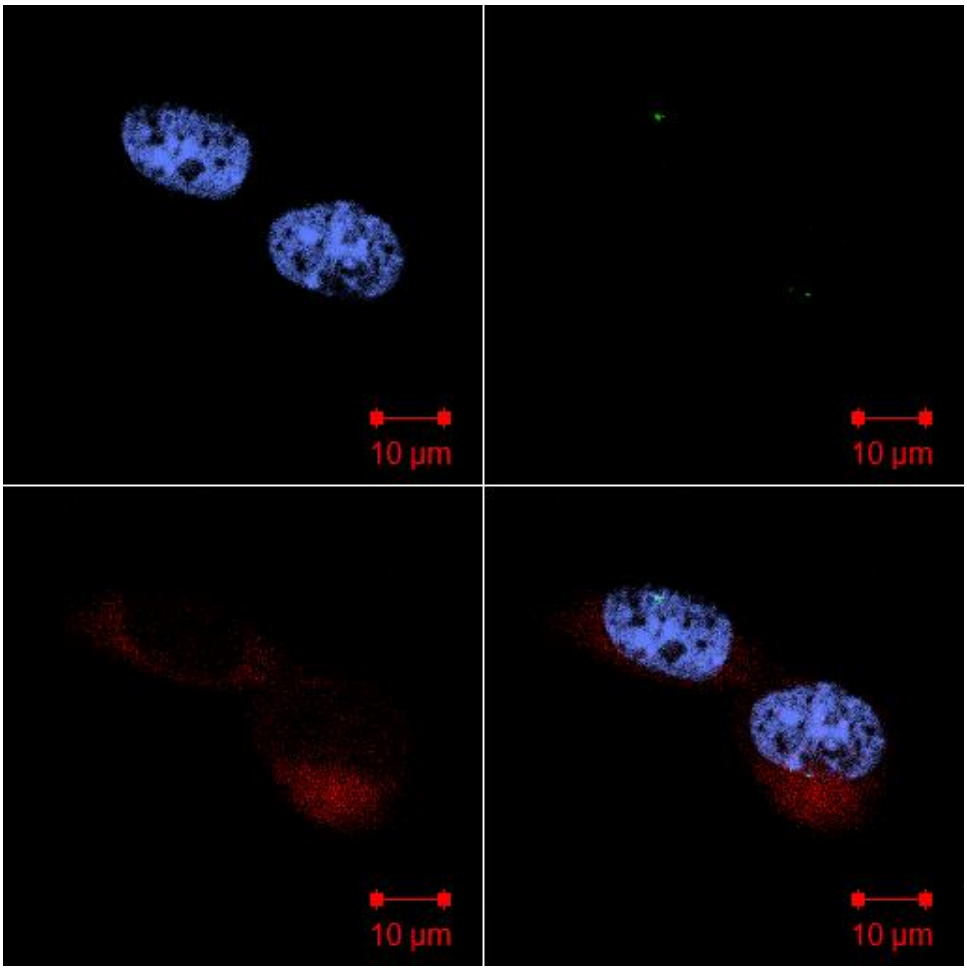

Figure 28. A micrograph of a fixed CHO-human hybrid cell line GM13535 showing non-disjunction in a daughter pair. DNA (upper left) is labeled with DAPI, chromosome 21 is label by *in situ* hybridization with green fluorophore probe to the 21p11.1-q11.1 chromosome region (upper right), microtubules are labeled with anti-tubulin antibody (lower left), and composite image (lower right). Scale bar represents 10µm.

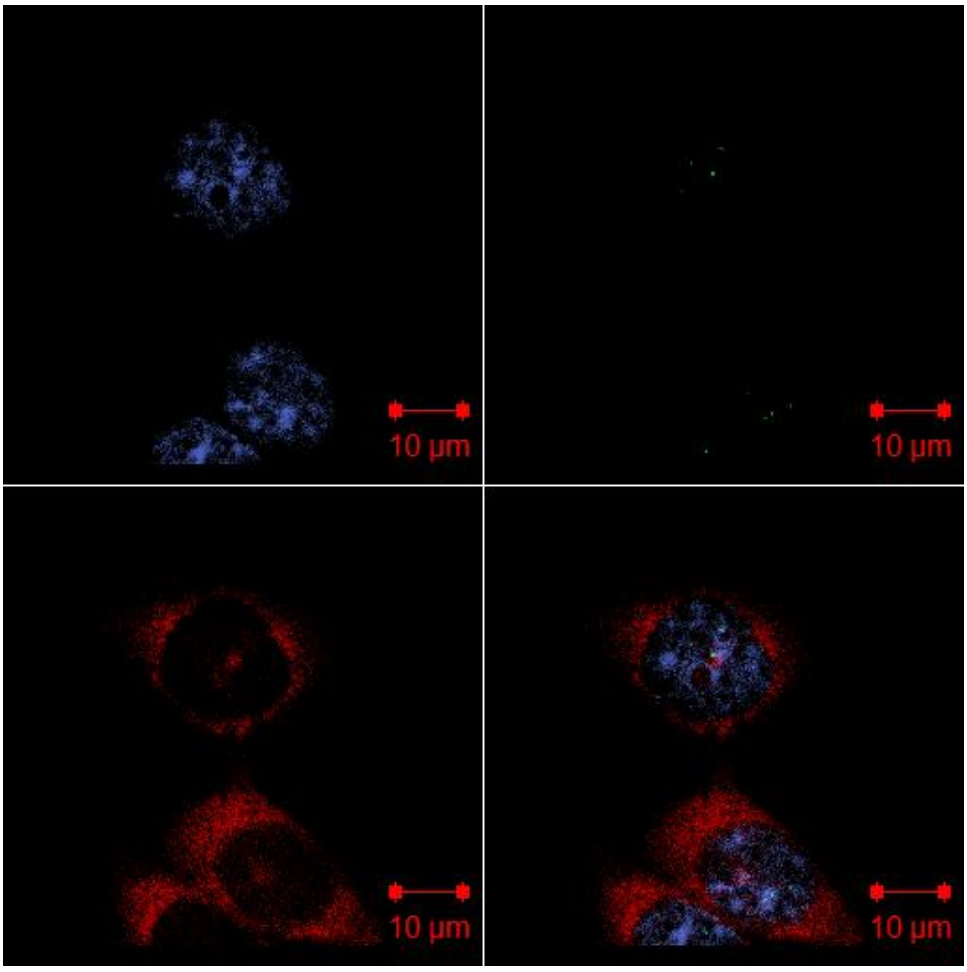

Figure 29. A micrograph of a fixed CHO-human hybrid cell line GM13535 showing correct segregation in a daughter pair. DNA (upper left) is labeled with DAPI, chromosome 21 is label by *in situ* hybridization with green fluorophore probe to the 21p11.1-q11.1 chromosome region (upper right), microtubules are labeled with anti-tubulin antibody (lower left), and composite image (lower right). Scale bar represents 10µm.

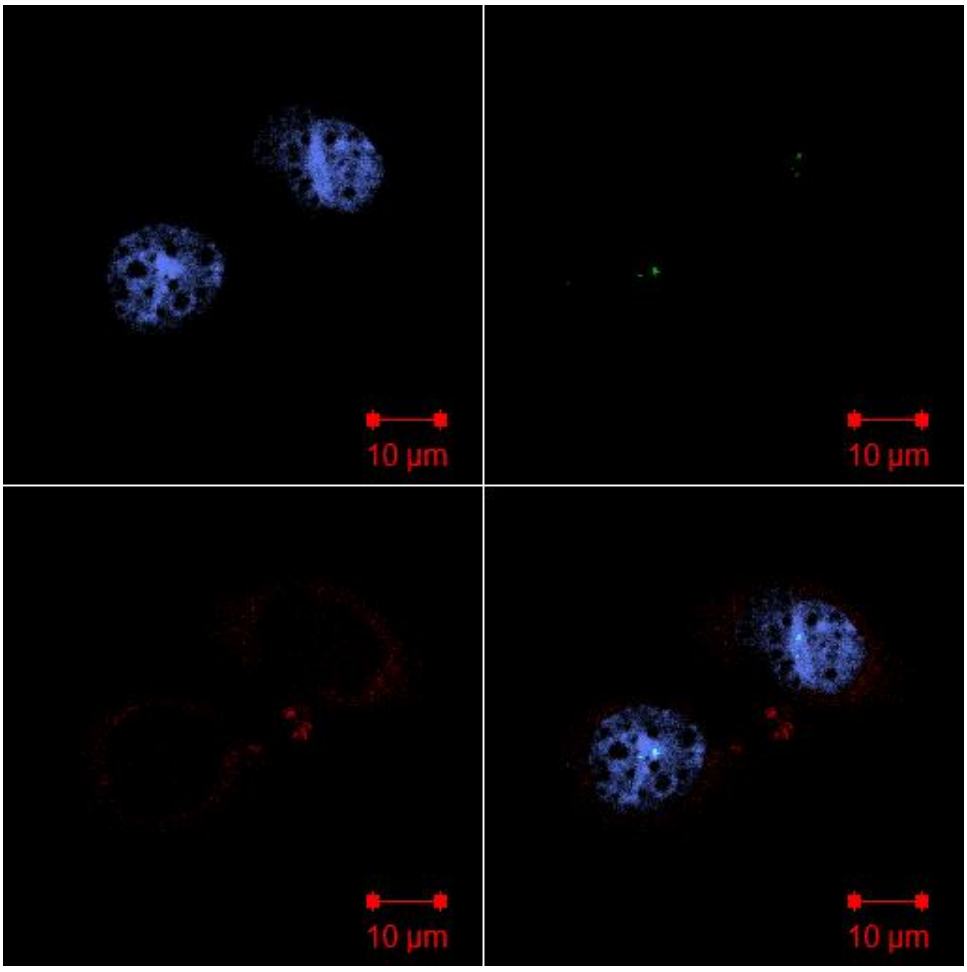

Figure 30. A micrograph of a fixed CHO-human hybrid cell line GM13535 showing correct segregation in a daughter pair. DNA (upper left) is labeled with DAPI, chromosome 21 is label by *in situ* hybridization with green fluorophore probe to the 21p11.1-q11.1 chromosome region (upper right), microtubules are labeled with anti-tubulin antibody (lower left), and composite image (lower right). Scale bar represents 10µm.

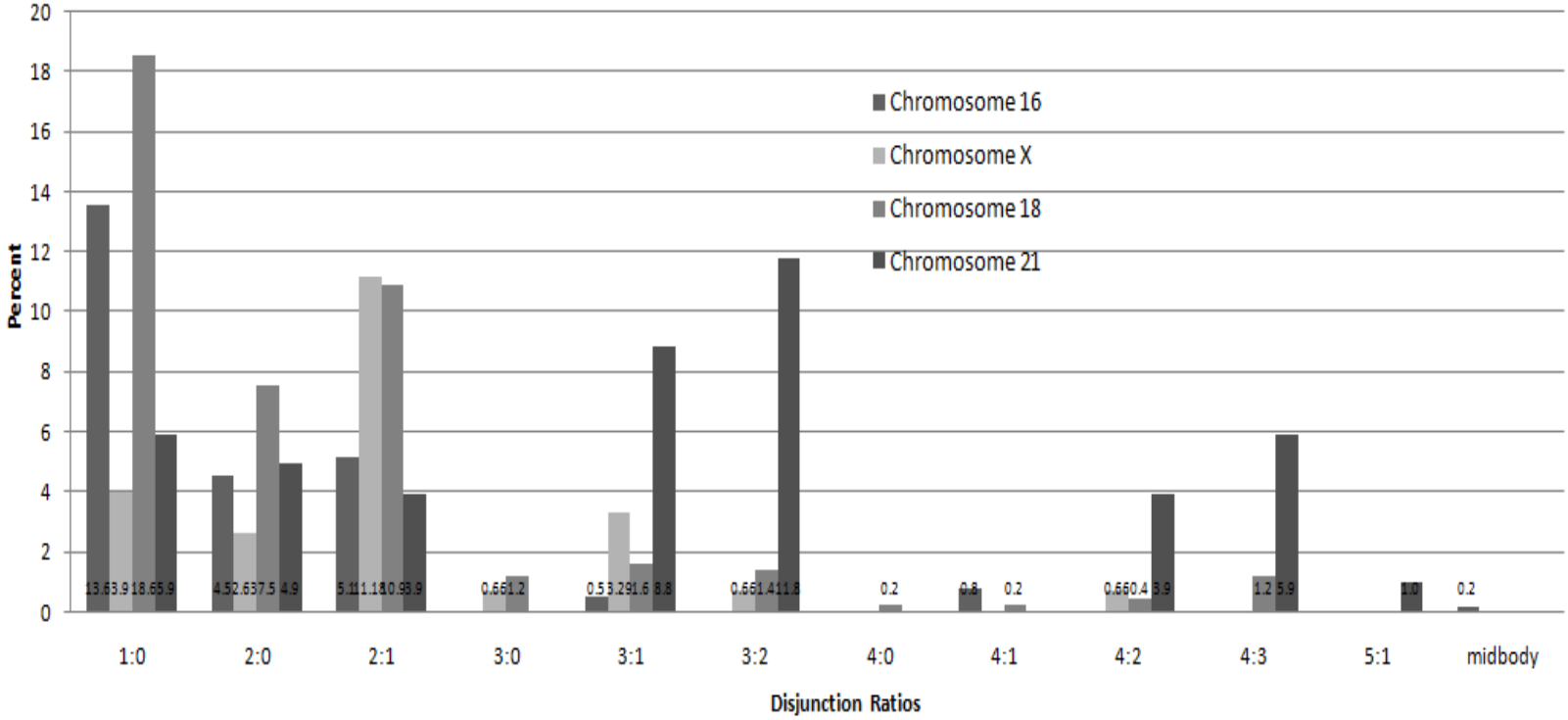

Figure 31. Intrinsic Rate of Different Non-disjunction Patterns by Chromosome

NOTE: Graph comparing the intrinsic rates of the different types of non-disjunction between chromosomes 16, 18, and X.

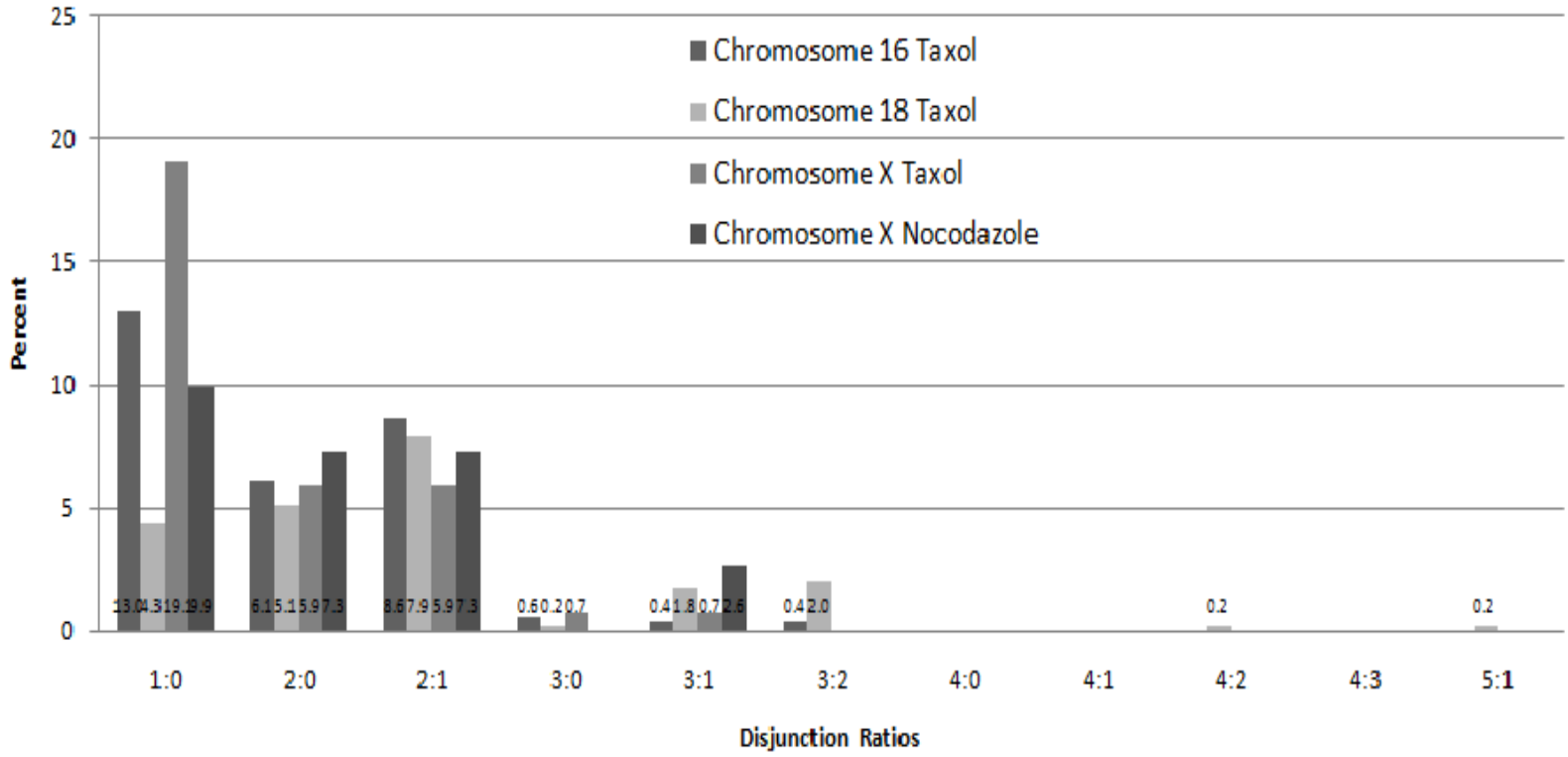

Figure 32. Effects of Microtubule Perturbation on Patterns of Non-disjunction

NOTE: Graph comparing the non-disjunction ratios of different chromosomes when they are treated with taxol or nocodazole.

Table 2. Odds Ratios for Intrinsic Rate of Non-disjunction

		Type 2 (Correct Disjunction of Chromosomes			
Type 1 (Non-disjunction of Chormosomes)		16	X	18	21
	16		0.92	2.31*	2.24*
	X	1.09		2.51*	2.44*
	18	0.43*	0.40*		0.97
	21	0.45*	0.41*	1.03	

NOTE: Table showing the odds ratios for the intrinsic rate of non-disjunction. Type 1 is the non-disjunction of chromosomes and type 2 is correct disjunction of chromosomes. The astrics denote significant difference.

CHAPTER IV

DISCUSSION

The maintenance of proper chromosome number in somatic cells depends on the precision of chromosome separation during mitosis. However, chromosome separation is not completely infallible. It is important to understand the mechanism of the failed separation. The goal of this research was to illuminate the mechanism of human chromosome separation using CHO-human hybrid cells as a model. This was accomplished by studying CHO-human hybrid cell lines containing chromosomes X, 21, 16, or 18, which provided a comparison among different chromosome in a standard cellular environment. We also established the intrinsic rate of non-disjunction in control cells. This allowed us to compare the intrinsic rate of non-disjunction with those in cells presented with a mitotic challenge.

Hybrid cells were treated with drugs such as nocodazole and taxol that perturbed microtubule turn over. Nocodazole promotes net disassemble and taxol promotes net assembly of spindle microtubules. An additional mitotic challenge can be induced by creating mitotic cells with unreplicated genomes (MUG). This was induced by treatment of the hybrid cells with the drugs, hydroxyurea and caffeine in order to inhibit replication of the chromosomes and to over ride the synthesis checkpoint and force cells into unscheduled mitosis. In each case, non-disjunction rates were measured using

centromere-specific fluorescence in situ hybridization (FISH) probes. Anti-tubulin antibody was used to identify daughter pair by revealing the midbody connecting them. The number of centromere signals in each daughter was then assayed. More specifically, the MUG experiment showed how chromosomes separate when their kinetochores and DNA are fragmented.

Chromosome separation is an event that many scientists have tried to understand for many years. Chromosome missegregation can lead to aneuploidy, which happens in many organisms and has been connected to many different cancers and medical conditions such as Down's syndrome in humans. These experiments provided new data on the frequency with which chromosomes are passed to daughter cells, and provided the intrinsic rate for individual chromosome separation. More specifically, the MUG experiment showed how chromosomes separate when their kinetochores and DNA are unreplicated and fragmented. In addition, the MUG experiment allowed us to analyze the kinetochore without chromosomal DNA. This is important because it provided insight into how human kinetochores segregate when their DNA is damaged. These experiments also measured how kinetochores react when put under different environmental stressors such as taxol and nocodazole, and provided, for the first time, some indication about whether or not some chromosomes are more prone to non-disjunction than are others.

Our data show that there is a difference in the intrinsic rate of non-disjunction between chromosomes. The four chromosomes could be divided into two groups based on their overall non-disjunction rates: Chromosomes 16 and X had approximately the same rate of non-disjunction and chromosomes 18 and 21 had approximately the same rate of non-disjunction. However, the non-disjunction ratios between all the

chromosomes differed. We found that chromosomes 18 and 21 were more prone to non-disjunction compared to chromosomes 16 and X. Maintenance of the kinetochore-microtubule connection and the orientation of the kinetochore are possible factors for the difference in the overall non-disjunction rates between the two groups. If the microtubules are not connected properly to the kinetochore, then this can cause a loss of tension which can lead to non-disjunction of the chromosomes. A difference in non-disjunction between chromosomes can be due to the efficiency at which separase cleaves cohesin between the two sister chromatids. If there is a defect in cleavage of sister chromatids then the sister chromatids cannot separate, leading to non-disjunction. In addition, they might separate and migrate to spindle poles early.

Chromosomes 16 and 18 were found to lose a chromatid more frequently than chromosomes X and 21. This could be caused by a decrease in the number of microtubules captured. In addition, congression of the chromosome to the equator can cause an increase in the loss of a chromatid. Also, kinetochore orientation can lead to a loss in a sister chromatid by not allowing microtubules to connect to the kinetochore. For example, if the kinetochores are oriented in a way that the sister kinetochores overlap, it can lead to a decrease in microtubule connects which may cause a loss in a chromatid. Chromosomes 18 and 21 non-disjoin the same overall, however, they undergo non-disjunction for different reasons. Chromosome 18 could be more prone to lose a chromatid prematurely before the spindle assembly checkpoint (SAC). This was illustrated in figure 31. Data showed that chromosome 18 had a higher frequency of 1:0 ratios demonstrating that chromosome 18 is more prone to losing a chromatid.

Microtubule perturbation with taxol led to an increase in non-disjunction for chromosomes 16 and X which may explain the reoccurrence of cancer after several rounds of chemotherapy. However, taxol decreased the rate of non-disjunction for chromosomes 18. This may be caused by the maintenance in kinetochore connection or capture of microtubules. In addition, chromosome 18 may have a decrease in the amount of microtubules captured. We propose that when taxol halts the cells during the SAC, it may allow more time for checkpoint proteins to repair the kinetochore-microtubule connection leading to a decrease in the rate of non-disjunction for chromosome 18. Chromosomes 16 and X may have an increase in the frequency of non-disjunction because they may non-disjoin before the SAC. Therefore, we propose that SAC may not detect the non-disjunction if the chromatid detaches before the SAC. We propose that chromosomes 16 and X may also be more prone to losing microtubule connections if the microtubules are stabilized for long periods of time. Chromosomes 16 and X may possibly have the same defect while the microtubules are perturbed because chromosomes 16 and X fall into the same group for the overall intrinsic rate of non-disjunction. For chromosome X, nocodazole had the same effect as taxol by increasing the overall rate of non-disjunction.

The MUG experiment was performed for chromosome 16. It showed how chromosomes react when their DNA is fragmented. *In situ* signals located in the midbody of the daughter pair indicated that non-disjunction occurred. Our data indicates that only 1.2% of cells had a signal in the midbody of a daughter pair. This indicates that even when the DNA is fragmented, the kinetochore will successfully disjoin most of the

time. We propose that DNA can still segregate properly even when DNA is damaged by environmental factors.

We propose that the difference in spindle assembly checkpoint protein genes found on different chromosomes can lead to the differences in non-disjunction among the chromosomes in a hybrid system. For example, isoforms of kinesin and dynein are found on chromosomes 16 and X however, it is not found on chromosomes 18 and 21 (Figures A.4 and A.5). This may possible explain how, in our four chromosomes, the chromosomes fall into two groups. In addition, spindle assemble protein concentration may influence the difference in non-disjunction among the different chromosomes. To rule out this possibility, this experiment can be performed using the Y chromosome since it does not contain any SAC protein genes. We propose that if there is a difference in protein concentration than that may possible lead to a decrease in efficiency of the SAC and the kinetochore-microtubule connection. In addition, the Y chromosome does not contain any proteins that are associated with spindle assembly, whereas the X chromosome contains genes that code for CENPI, p55, dynein, kinesin, EB1, and cohesin (Figures A.4 and A.5).

The CHO-human hybrid system may also influence the rate of non-disjunction of the chromosomes. We propose that an increase in non-disjunction may occur when the CHO kinetochore proteins interfere with the human kinetochore proteins that are encoded by the human chromosome. However, this would allow the non-disjunction rate to increase to frequency that will allow investigators to detect the non-disjunction and compare them to microtubule perturbed cells.

CHAPTER V

CONCLUSIONS

We have shown that four human chromosomes have very different intrinsic rates of non-disjunction. Chromosomes 16 and X behave in a similar way, both with regard to the intrinsic non-disjunction rate as well as the response to microtubule perturbation. Likewise, chromosomes 18 and 21 have much higher intrinsic rates of non-disjunction and respond to microtubule perturbation in a different way. For example, the rate of non-disjunction for chromosome 18 decreases when microtubules are perturbed by taxol. Our results strongly imply that human chromosomes cannot be thought of as behaving in similar ways to mitotic challenges, or even to the vicissitudes of aging in cell lineages. We anticipate that these experiments will provide a way in which to take a closer look at human chromosome mitotic performance and might shed light on the on-going question of the contribution of aneuploidy to cancer and possible prevention of meiotic non-disjunction syndromes.

LITERATURE CITED

Bakou, K.; G. Stephanou; C. Andrianopoulos; and N. A. Demopoulos. (2002). Spontaneous and spindle poison-induced micronuclei and chromosome non-disjunction in cytokinesis-blocked lymphocytes from two age groups of women. Mutagenesis 17: 233-39.

Carere, A.; A. Antoccia; D. Cimini; R. Crebelli; F. Degrassi; P. Leopardi; F. Marcon; A. Sgura; C. Tanzarella; and A. Zijno. (1999). Analysis of chromosome loss and non-disjunction in cytokinesis-blocked lymphocytes of 24 male subjects. Mutagenesis 14: 491-96.

Cimini, D.; and F. Degrassi. (2005). Aneuploidy: a matter of bad connections. Trends Cell Biol 15: 442-51.

Cimini, D.; B. Moree, J; C. Canman; and E. D. Salmon. (2003). Merotelic kinetochore orientation occurs frequently during early mitosis in mammalian tissue cells and error correction is achieved by two different mechanisms. J Cell Sci 116: 4213-225.

Cimini, D.; B. Howell; P. Maddox; A. Khodjakov; and F. Degrassi. (2001). Merotelic kinetochore orientation is a major mechanism of aneuploidy in mitotic mammalian tissue cells. J Cell Biol 153: 517-27.

Cimini, D.; C. Tanzarella; and F. Degrassi. (1999). Differences in malsegregation rates obtained by scoring ana-telophases or binucleated cells. Mutagenesis 14: 563-68.

Cimini, D.; D. Fioravanti; E. D. Salmon; and F. Degrassi. (2002). Merotelic kinetochore orientation versus chromosome mono-orientation in the origin of lagging chromosomes in human primary cells. J Cell Sci 115: 507-15.

Coelho, P. A.; J. Queiroz-Machado; A.M. Carmo; S. Mountinho-Pereira; H. Maiato; and C. E. Sunkel. (2008). Dual role of topoisomerase II in centromere resolution and aurora b activity. PLoS Biol 6: 1758-1777.

Diego-Alvarez, D.; C. Ramos-Corrales; M. Garcia-Hoyos; A. Bustamente-Aragones; Diego Cantalapiedra; Joaquin Diaz-Recasens; Elena Vallespin-Garcia; Carmen Ayuso; and Isabel Lorda-Sanchez. (2005). Double trisomy in spontaneous miscarriages: cytogenetics and molecular approach. Hum Reprod 21: 958-966.
Fant, X.; A. Merdes; and L. Haren. (2004). Cell and molecular biology of spindle poles and NuMA. Int Rev Cytol 238: 1-57.

Hall, H.; P. Hunt; and T. Hassold. (2006). Meiosis and sex chromosome aneuploidy: how meiotic errors cause aneuploidy; how aneuploidy causes meiotic errors. Curr Opin Genet Dev 16: 323-329.

Hassold, T.; H. Hall; and P. Hunt. (2007). The origin of human aneuploidy: where we have been, where we are going. Hum Mol Genet 16: R203-208.

Hornick, J.E.; J.R. Bader; E.K. Tribble; K. Trimble; J.S. Breunig; E.S. Halpin; K.T. Vaughan; and E.H. Hinchcliffe. (2008). Live-cell analysis of mitotic spindle formation in taxol-treated cells. Cell Motil Cytoskeleton 65: 595-613.

Ikui, A.E.; C.P.H.Yang; T. Matsumoto; and S.B. Horwitz. (2005). Low concentrations of taxol cause mitotic delay followed by premature dissociation of p55CDC from Mad2 and BubR1 and abrogation of the spindle checkpoint, leading to aneuploidy. Cell Cycle 4: 1385-1388.

Martin, R. H.; and A. W. Rademaker. (1999). Non-disjunction in human sperm: comparison of frequencies in acrocentric chromosomes. Cytogenet Cell Genet 86: 43-45.

Nicklas, R. B. (1988). Chromosome and kinetochores do more in mitosis than previously thought. Chromosome Structure and Function: The Impact of New Concepts: 53-74.

Pellman, D. (2007). Aneuploidy and cancer. Nature 446: 38-39.

Salmon, E. D.; D. Cimini; L. A. Cameron; and J. G. DeLuca. (2005). Merotelic kinetochores in mammalian tissue cells. Philos Trans R Soc Lond B Biol Sci B 360: 553-68.

Sudakin, V.; and T. J. Yen. (2007). Targeting mitosis for anti-cancer therapy. Biodrugs 21: 225-33.

Sun, Q. Y.; and H. Schatten. (2007). Centrosome inheritance after fertilization and nuclear transfer in mammals. Adv Exp Med Biol 591: 58-71.

Tanaka, T. U.; and A. Desai. (2008). Kinetochore-microtubule interactions: the means to the end. Curr Opin Cell Biol 20: 53-63.

Thomas, N.S.; S. Ennis; A.J. Sharp; M. Durkie; T. J. Hassold; A. R. Collins; and P. A. Jacobs. (2001). Maternal sex chromosome non-disjunction: evidence for X chromosome-specific risk factors. Hum Mole Gen 10:243-250.

Thompson, S. L.; and D. A. Compton. (2008). Examining the link between chromosomal instability and aneuploidy in human cells. J cell Biol 180: 665-672.

Wise, D. A.; and B. R. Brinkley. (1997). Mitosis in cells with unreplicated genomes (MUGs): spindle assembly and behavior of centromere fragments. Cell Motil Cytoskeleton 36: 291-302.

Varma, D.; P. Monzo; S. A. Stehman; and R. B. Vallee. (2008). Direct role of dynein motor in stable kinetochore-microtubule attachment, orientation, and alignment. J Cell Biol 182: 1045-1054.

Verdoodt, B.; I. Decordier; K. Geleyns; M. Cunha; E. Cundari; and M. Kirsch-Volders. (1999). Induction of polyploidy and apoptosis after exposure to high concentrations of the spindle poison nocodazole. Mutagenesis 14: 513-520.

Yen, T. J.; S. A. Jablonski; S.T. Liu; V. Sudakin; Y.C. Li; S. Teppone; J. Feng; D. P Matheos; N. Ladygina; E. A. Skorichenko; J. Hittle; B. J. Conner; N. Tikhmyanova; and M. Du. (2004). Molecular mechanisms that maintain genome stability in human cells. Fox Chase Cancer Center 2004 Scientific Report: 1-5.

Zhao, Lian; K. Hayes; Z. Khan; A. Glassman. (2001). Spectral karyotyping study of chromosome abnormalities in human leukemia. Cancer Gene Cytogenet 127: 143-147.

APPENDIX A

INTERCHROMOSOME STATISTICAL DATA ANALYSIS AND SPINDLE ASSEMBLY CHECKPOINT GENE ANALYSIS

Nominal Logistic Fit for Segregation Type

Freq: Frequency

Whole Model Test

Model	-LogLikelihood	DF	ChiSquare	Prob>ChiSq
Difference	8.03673	3	16.07347	0.0011*
Full	246.06934			
Reduced	254.10608			

RSquare (U)	0.0316
Observations (or Sum Wgts)	400

Converged by Gradient

Parameter Estimates

Term	Estimate	Std Error	ChiSquare	Prob>ChiSq	Lower 95%	Upper 95%
Intercept	0.73313556	0.1096144	44.73	<.0001*	0.52112022	0.95133425
Chromosome[16]	0.38971861	0.1975099	3.89	0.0485*	0.01103737	0.78797501
Chromosome[18]	-0.4466062	0.1800795	6.15	0.0131*	-0.7993148	-0.0920503
Chromosome[21]	-0.4167982	0.1803326	5.34	0.0208*	-0.769785	-0.061508

For log odds of Correct Segregation/Non-Disjunction

Effect Wald Tests

Source	Nparm	DF	Wald ChiSquare	Prob>ChiSq
Chromosome	3	3	15.5578218	0.0014*
Treatment	0	0	.	.
Chromosome*Treatment	0	0	.	.

Effect Likelihood Ratio Tests

Source	Nparm	DF	L-R ChiSquare	Prob>ChiSq
Chromosome	3	3	16.0734674	0.0011*
Treatment	0	0	.	.
Chromosome*Treatment	0	0	.	.

Odds Ratios

For Segregation Type odds of Correct Segregation versus Non-Disjunction

Odds Ratios for Chromosome

Level1	/Level2	Odds Ratio	Reciprocal
18	16	0.4333	2.3078696
21	16	0.4464103	2.2400918
21	18	1.0302567	0.9706319
X	16	1.0875933	0.9194614
X	18	2.5100234	0.3984027
X	21	2.4363088	0.410457

Prediction Profiler

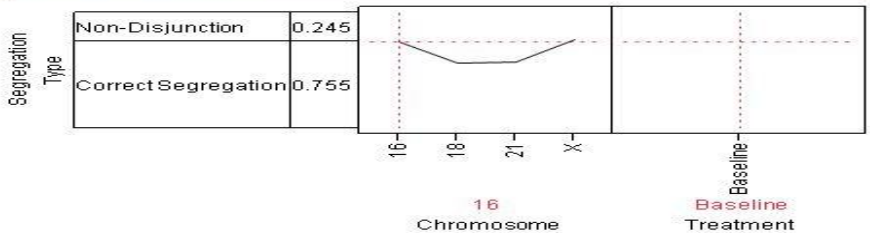

Figure A.1 Nominal Logistic Fit for the Intrinsic Rate of Disjunction of Chromosomes

NOTE: The figure above illustrates the output data to the question does the type of chromosome has an effect on distribution (correct disjunction vs. Non-disjunction) for cells without a treatment (intrinsic rate).

Nominal Logistic Fit for Segregation Type

Freq: Frequency

Whole Model Test

Model	-LogLikelihood	DF	ChiSquare	Prob>ChiSq
Difference	5.22908	1	10.45816	0.0012*
Full	120.54770			
Reduced	125.77678			
RSquare (U)	0.0416			
Observations (or Sum Wgts)	200			

Converged by Gradient

Parameter Estimates

Term	Estimate	Std Error	ChiSquare	Prob>ChiSq	Lower 95%	Upper 95%
Intercept	0.78624543	0.1579335	24.78	<.0001*	0.48297052	1.10377787
Treatment[Baseline]	-0.4997161	0.1579335	10.01	0.0016*	-0.8158558	-0.194799

For log odds of Correct Segregation/Non-Disjunction

Effect Wald Tests

Source	Nparm	DF	Wald ChiSquare	Prob>ChiSq
Chromosome	0	0	.	.
Treatment	1	1	10.011481	0.0016*
Chromosome*Treatment	0	0	.	.

Effect Likelihood Ratio Tests

Source	Nparm	DF	L-R ChiSquare	Prob>ChiSq
Chromosome	0	0	.	.
Treatment	1	1	10.4581568	0.0012*
Chromosome*Treatment	0	0	.	.

Odds Ratios

For Segregation Type odds of Correct Segregation versus Non-Disjunction

Odds Ratios for Treatment

Level1	/Level2	Odds Ratio	Reciprocal
Taxol	Baseline	2.7167388	0.3680884

Receiver Operating Characteristic

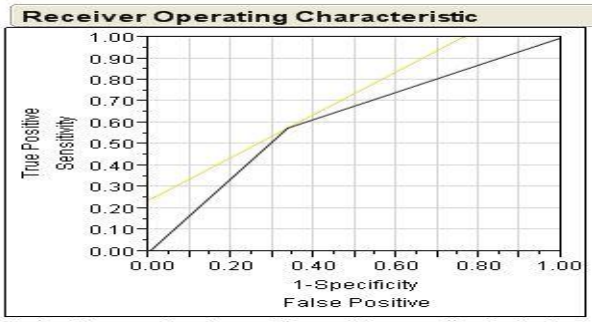

Using Segregation Type='Correct Segregation' to be the positive level

Area Under Curve = 0.62143

Lift Curve

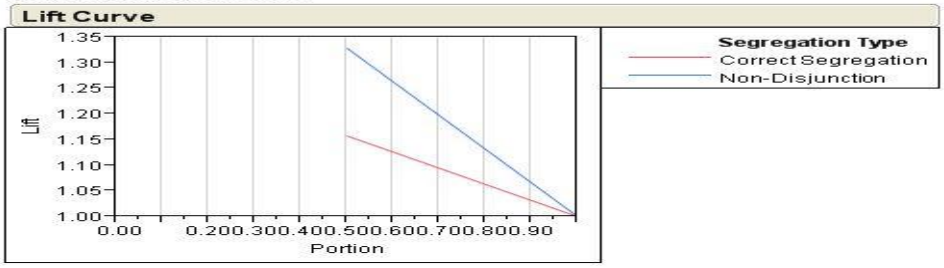

Figure A.2 Nominal Logistic Fit for Disjunction of Chromosomes Treated with Taxol

NOTE: The figure above illustrates the output data to the question does the different treatments (intrinsic vs. taxol) have an effect on non-disjunction for chromosome 18.

Nominal Logistic Fit for Segregation Type

Freq: Frequency

Whole Model Test

Model	-LogLikelihood	DF	ChiSquare	Prob>ChiSq
Difference	10.77378	6	21.54756	0.0015*
Full	421.53982			
Reduced	432.31360			

RSquare (U) 0.0249
Observations (or Sum Wgts) 700
Converged by Objective

Parameter Estimates

Term		Estimate	Std Error	ChiSquare	Prob>ChiSq	Lower 95%	Upper 95%
Intercept	Biased	0.78308173	0.0886976	77.95	<.0001*	.	.
Chromosome[16]	Biased	0.22450609	0.1445946	2.41	0.1205	.	.
Chromosome[18]	Biased	0.0031637	0.1399422	0.00	0.9820	.	.
Chromosome[21]	Biased	-0.4167982	0.1803326	5.34	0.0208*	.	.
Treatment[Baseline]	Biased	-0.0499462	0.0919508	0.30	0.5870	.	.
Chromosome[16]*Treatment[Baseline]	Biased	0.16521252	0.1303693	1.61	0.2051	.	.
Chromosome[18]*Treatment[Baseline]	Biased	-0.4497699	0.1294962	12.06	0.0005*	.	.
Chromosome[21]*Treatment[Baseline]	Zeroed	0	0	99999	0.0000*	.	.

For log odds of Correct Segregation/Non-Disjunction

Effect Wald Tests

Source	Nparm	DF	Wald ChiSquare	Prob>ChiSq	
Chromosome	3	3	6.2385741	0.1006	
Treatment	1	1	0.29504852	0.5870	
Chromosome*Treatment	3	2	12.3457727	0.0021*	LostDFs

Effect Likelihood Ratio Tests

Source	Nparm	DF	L-R ChiSquare	Prob>ChiSq
Chromosome	3	3	1.11267651	0.7740
Treatment	1	1	0	1.0000
Chromosome*Treatment	3	2	12.714092	0.0017*

Odds Ratios

For Segregation Type odds of Correct Segregation versus Non-Disjunction

Odds Ratios for Chromosome

Level1	/Level2	Odds Ratio	Reciprocal
18	16	0.8014422	1.2477506
21	16	0.5266051	1.8989561
21	18	0.6570718	1.5219036
X	16	0.9652408	1.0360109
X	18	1.2043798	0.8303029
X	21	1.83295	0.5455686

Odds Ratios for Treatment

Level1	/Level2	Odds Ratio	Reciprocal
Taxol	Baseline	1.1050519	0.9049348

Receiver Operating Characteristic

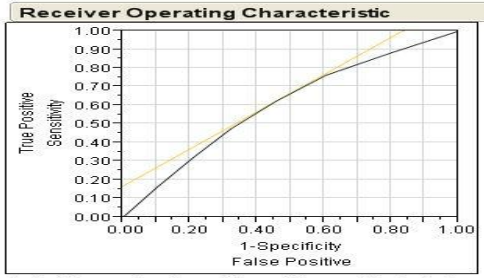

Using Segregation Type='Correct Segregation' to be the positive level

Area Under Curve = 0.60508

Lift Curve

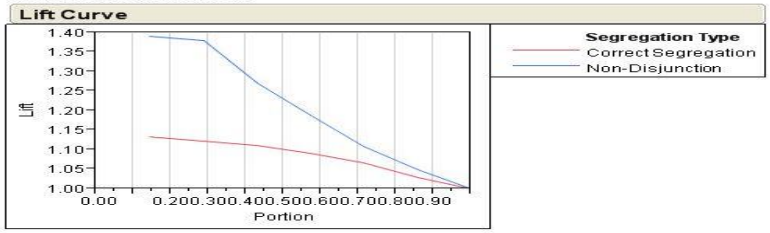

Figure A.3 Nominal Logistic Fit for Disjunction of Chromosomes 16, X, 18, and 21

NOTE: The figure above illustrates the output data to the question does the different treatments (intrinsic vs. taxol) have an effect on non-disjunction.

Table A.1 Location of Proteins Associated with the Spindle Assembly Checkpoint

Proteins Associated with the Spindle Assembly Checkpoint	Chromosome(s) where Protein is Located
Mitotic Spindle Assembly Checkpoint	7, 22
BUB1	2, 15
CENPA	2
CENPB	14
CENPC	4
CENPH	5
CENPI	X
hMIS12	17
MAD1	2, 4, 7, 22
MAD2	1, 4, 6, 10, 14, 18
BUBR1	15
BUB3	7, 10, 20
CDC20	1, 5, 9, 19
p55	1, 2, 7, 10, 12, 14, 17, 19, 20, 21, 22, X
CDC27	17
APC3	17
dynein	1, 2, 3, 5, 6, 7, 8, 9, 10, 11, 12, 14, 16, 17, 20, 22, X
dynactin	1, 2, 5, 8, 9, 12, 16, 17
MCAK	1
kinesin	1, 2, 3, 5, 6, 8, 9, 10, 11, 12, 14, 15, 16, 17, 19, 20, X
Ndc80	1, 2, 18, 19
Dam1	1
EB1	1, 2, 3, 4, 5, 6, 7, 8, 9, 10, 11, 12, 13, 14, 15, 16, 17, 18, 19, 20, 21, 22, X
Aurora-B	8, 11, 17
INCENP	11
cohesin	7, 10, X

NOTE: The chart above shows the different proteins associated with the spindle assembly checkpoint and the chromosomes on which the gene is located.

Table A.2 Spindle Assembly Checkpoint Proteins Located on Chromosomes 16, X, 18, and 21

Chromosome where Protein is Located	Proteins Associated with the Spindle Assembly Checkpoint
16	dynein, dynactin, kinesin, EB1
X	CENPI, p55, dynein, kinesin, EB1, cohesin
18	MAD2, Ndc80, EB1
21	p55, EB1

NOTE: The chart above shows the chromosomes relevant to our study and the different proteins associated with the spindle assembly checkpoint.